1969

An experimental investigation of the velocity and heat generation characteristics of a fixed boundary fracture model

Thomas L. Paxson
Lehigh University

AN EXPERIMENTAL INVESTIGATION OF THE VELOCITY AND HEAT GENERATION CHARACTERISTICS OF A FIXED BOUNDARY FRACTURE MODEL

by

Thomas Lanard Paxson

A THESIS

Presented to the Graduate Faculty

of Lehigh University

in Candidacy for the Degree of

Master of Science

in

Mechanical Engineering

Lehigh University

1969

CERTIFICATE OF APPROVAL

This thesis is accepted and approved in partial fulfillment of the requirements for the degree of Master of Science.

April 14, 1969
(date)

Robert A Lucas
Professor in Charge

Ferdinand F. Bell
Chairman of the Department

ACKNOWLEDGEMENTS

I want to thank Robert A. Lucas, Ph.D., for his endless patience and support, William A. Barrett, Ph.D., for his invaluable aid in the electronic area, especially for his design of the electronic timer. His efforts and the cooperation of the faculty and staff of the Electrical Engineering Department made the development of this timer possible. Professor Thomas E. Jackson and machinist Frank Pechacek provided advice and technical skill without which the experiment could not have been developed. Finally, I want to thank my Lord God without whose help, nothing is accomplished.

TABLE OF CONTENTS

LIST OF FIGURES

LIST OF TABLES

ABSTRACT

An experimental investigation of the fracture velocity characteristics of a quasi-brittle material under fixed boundary conditions has been conducted. In addition, an apparatus to measure the heat generated by a quasi-static, propagating crack has been designed.

Using models of 1/8 inch thick Plexiglas II (polymethyl methacrylate), the quasi-static character of the fracture velocity for the fixed boundary model has been verified, in the sense that for a fixed crack extension force, the velocity is a constant quantity. The magnitude of this velocity was measured and found to increase with increasing stress levels, to a terminal value in excess of 2180 ft./sec. This is in agreement with published theoretical and experimental values of 2330 ft./sec. and 2200 ft./sec., respectively.

An electronic timer, using commercial integrated circuits, has been designed and constructed for the above measurements. Designed for use with the velocity gage technique of velocity measurement, this instrument is capable of measuring the crack propagation time between ten successive current paths, each having a 32 to 1024μ sec. duration, with a resolution of $\pm$ 1 μsec. . In addition, the feasibility of measuring the fracture velocity over small, 1/2 to 1 inch, increments and investigating fracture acceleration with this device has been established.

I. INTRODUCTION

The examination of material behavior at the high failure rates is part of the larger effort to determine the mechanisms of unstable fracture. By analyzing these mechanisms and classifying them with respect to their magnitude of effect on a material's fracture rate, investigators hope to predict and control the failure rate of engineering materials. This thesis is a small contribution to the examination of this phenomenon. Specifically, it is the initial phase of an experimental investigation of the fixed boundary problem for quasi-brittle materials.

Experimental and analytical considerations of the crack velocity and heat generation in the explanation of material behavior for the simple tension, plane stress, model have been offered for the past two decades. In 1948, Mott [1]* presented an analysis of the dynamics of fracture based on an extension of Griffith's energy explanation of material failure. By including the kinetic energy associated with fracture in the energy balance, he developed the expression for the velocity of a central crack in an infinite sheet as follows;

$$\dot{a} = \left(\frac{2\pi}{k^{**}}\right)^{1/2} \left(\frac{E}{\rho}\right)^{1/2} \left(1 - \frac{a_o}{a}\right)^{1/2}$$

with the condition that $\frac{\partial \dot{a}}{\partial a} = 0$. Here, $\left(\frac{2\pi}{k^{**}}\right)^{1/2}$ is a numerical constant, $\left(\frac{E}{\rho}\right)^{1/2}$ is the elastic wave velocity and a_o and

*Numbers in brackets refer to references at end of paper.

a are the initial and instantaneous half crack lengths respectively. By 1954, Roberts and Wells [2] had numerically evaluated $(\frac{2\pi}{k^{**}})^{1/2}$ and had shown that the terminal crack velocity was related to the elastic wave velocity by

$$V_T = 0.38\,(\frac{E}{\rho})^{1/2} \quad *$$

where $V_T = (\frac{2\pi E}{k^{**}\rho})^{1/2}$. To substantiate their work, Roberts and Wells tabulated the results of the experimental efforts of seven other investigators (1938 - 1953). The terminal velocities and elastic wave velocities found in glass, fused quartz, steel, and cellulose acetate were listed along with the ratio of these velocities $(V_T/(E/\rho)^{1/2})$ which ranged from 0.20 for steel to 0.42 for fused quartz.

Dulaney and Brace (1960) [3] refined Mott's analysis. They first solved for the constant energy value, C_1, by applying the boundary condition for the velocity

$$\dot{a} = 0 \text{ when } a = a_o$$

to Mott's energy balance. They then substituted this value of C_1 into the energy equation and algebraically solved for $\dot{a}$, finding that:

*For $\nu = 0.25$ and large times $(t \to t_\infty)$.

$$\dot{a} = \left(\frac{2\pi}{k^{**}}\right)^{1/2} \left(\frac{E}{\rho}\right)^{1/2} \left(1 - \frac{a_o}{a}\right)$$

Comparing this velocity behavior with the crack propagation data for thin plexiglas sheets, accumulated by E. Orowan, they found that the experimental velocities approached their predicted terminal velocity, but, at a rate prescribed by an initial crack length 4 to 5 times greater than the actual value. The explanation offered by Dulaney and Brace, for this behavior, was that the heat generated during fracture (a quantity which decreases with increasing velocity and strain rate, according to Maxwell [4] (1959)) represented an energy loss of sufficient magnitude, at the low velocity levels, to cause the discrepancy.

In 1959, Manitz [5] also ran tensile fracture tests on plexiglas, measuring both the crack velocity and heat generation. He concluded that the heat generation (and loss) increases with fracture velocity due to the enlargement of the real fracture surface. He also stated that the increased surface roughness which occurred at high fracture speeds was a good indication of this enlargement. Later (1964 - 1965) Cotterell [6,7] conducted tests on large plexiglas sheets in simple tension and measured a terminal velocity of 2200 ft./sec. before branching occurred. He likewise noticed an increase in the fracture surface roughness with increasing crack velocity. Further, he concluded that there is a dependency

of the crack extension force, G, on the velocity of propagation, fracture length and applied stress and that the terminal velocity is related to the elastic wave velocity by

$$V_T = \frac{1}{3} \left(\frac{E}{\rho}\right)^{1/2}$$

for plexiglas.

Very little experimental work has been done on the fixed boundary problem. Song [8] (1960) has tested aluminum sheets and shown that decreasing the distance between the grips, as the crack grows, tends to arrest crack growth. Paris [9] (1955), and Paris and Whitmore [10] (1959) have also investigated the fixed boundary model but have not conducted extensive velocity tests.

The lack of experimental investigation of the fixed boundary problem, along with the constant velocity characteristics obtainable with the model thereby simplifying examination of material properties, have prompted its use in this investigation. Even with the extensive experimentation being conducted with the simple tensile model, the mechanisms of fracture have not been isolated. This, more than anything, emphasizes the need for a complete experimental investigation of a single model to erase the many uncertainties which now exist in the area.

Toward this end, the velocity meter principle has been combined with an electronic timer, providing versatility and accuracy never before available for velocity measurement. In addition, the basic design work for an apparatus to measure the heat generation associated with quasi-brittle fracture has been completed and summarized.

II. ANALYTICAL CONSIDERATIONS

The following definitions are basic to fracture mechanics in general, or, where noted, to the fixed boundary problems.

In the vicinity of the crack tip, for a case of plane stress, the stress components are:

$$\sigma_y = \frac{K}{(2\pi r)^{1/2}} \cos\frac{\theta}{2}\left(1 + \sin\frac{\theta}{2}\sin\frac{3\theta}{2}\right) \quad *$$

$$\sigma_x = \frac{K}{(2\pi r)^{1/2}} \cos\frac{\theta}{2}\left(1 - \sin\frac{\theta}{2}\sin\frac{3\theta}{2}\right) \qquad (1)$$

$$\tau_{xy} = \frac{K}{(2\pi r)^{1/2}} \cos\frac{\theta}{2}\sin\frac{\theta}{2}\cos\frac{3\theta}{2}$$

where the coordinates are defined in Figure 1a. K is called the "stress intensity factor" and is a function of the load level and configuration. For an infinite plate containing a semi-infinite crack with a uniform stress σ, first applied in the y-direction (perpendicular to the crack path) and then fixed boundaries clamped at $y = \pm h/2$, (see Figure 1b) K is defined by,

$$K = \frac{\sigma h^{1/2}}{2^{1/2}} \quad ** \qquad (2)$$

---

* Shannon, J. L., [11], p. 125.

** Paris, P. C., and Sih, G. C., [12], p. 71.

For the sake of brevity, such a configuration will be referred to in the future as the "fixed boundary problem". To satisfy the above qualifications, with a finite model, the following conditions must be satisfied:

$$h \ll b \tag{3a}$$

$$h < a < b-h \tag{3b}$$

Equation (3a) justifies the infinite plate assumption and Equation (3b) defines a "test section" for which the crack can be considered semi-infinite and in which the velocity of propagation is expected to be constant.

The fracture toughness, K_c, is a material property which represents the value of the stress intensity factor above which unstable fracture occurs. Once K_c is determined, for one model and load configuration, it is known for all configurations. Hence, the standard model for determining K_c is a plate of width 2b containing a central crack of length 2a, such that $a < b/2$. A uniform tensile stress is applied perpendicular to the crack until fracture occurs. The stress level and crack length, at the onset of unstable propagation, are substituted into the equation

$$K_c = \sigma(\pi a)^{1/2} \left(\frac{2b}{\pi a} \tan \frac{\pi a}{2b}\right)^{1/2} \quad (4)$$

*

where the final term is a width correction factor, to determine K_c.

The crack extension force, G(in./lb.), is "the unrecoverable loss of stress-field energy per unit area of crack extension"**. It is synonymous with the strain (or elastic) energy release rate, dG/dA, and, for a crack of length, 2a, in an infinite sheet with uniaxial tension stress, σ, perpendicular to the crack, it has a value:

***

$$G = \frac{\pi\sigma^2 a}{E} \quad (5)$$

where E is Young's modulus. For this same case,

****

$$K = \sigma\sqrt{\pi a} \quad (6)$$

hence, the crack extension force, G, is related to the stress intensity factor, K, by

$$G = \frac{K^2}{E} \quad (7)$$

---

* Paris, P. C., and Sih, G. C., [12], p. 35.

** Irwin, G. R., and Clark, A. B. J., [13], p. 322.

*** Paris, P. C., and Whitmore, C. F., [10], p. 1.

**** Paris, P. C., and Sih, G. C., [12], p. 33.

Paris and Whitmore [10] have shown that for the fixed boundary problem;

$$G = \frac{\sigma^2 h}{2E} \quad (8)$$

*

which is also

$$G = \frac{K^2}{E} \quad (9)$$

The heat associated with unstable fracture cannot be measured directly, however, it is known to be a function of temperature which is directly measurable. To establish meaningful design criterions, this relation must first be known, hence, a brief explanation of the analytical model and derivation of the temperature-heat equation follows.

The heat, with which this experiment is concerned, is generated in a small region immediately preceding the crack tip by the irreversible work associated with the plastic deformation in that area. This zone can be approximated by an instantaneous strip heat source along the crack face, since:

1. At any time, t, during the crack propagation, the small region of heat generation may be approximated by an instantaneous line source, of length, z, (where z is the plate thickness) perpendicular to the plate surfaces.

*Paris, P. C., and Whitmore, C. F., [10], p. 5.

2. The velocity of crack propagation, (also the velocity at which the above line source travels), is much, much greater than velocity of the thermal waves through the material.

The following solution of the instantaneous strip source problem follows that of Manitz [5] and is also presented in Carslaw and Jaeger [14].

The heat conduction equation is

$$\frac{\partial U}{\partial t} = a^* \frac{\partial^2 Y}{\partial t^2} \tag{10}$$

where, U is the temperature, t is time, a^* is the thermal diffusivity defined as, $\lambda/\rho c$, where λ is the thermal conductivity, ρ is the density and c is the specific heat, and x is the distance from the heat source. The solution of Equation (10) for a strip source is

$$U(x,t) = \frac{Q_F}{c\ \rho\sqrt{4\pi a^* t}}\, e^{-\frac{x^2}{4a^* t}} \tag{11}$$

where Q_F is the heat generated per unit length and x is the distance from the crack face (heat source) measured perpendicular to that face. The crack face is designated as the x = 0 plane.

At a distance, d, from the crack face,

$$U(d,t) = \frac{Q_F}{c\ \rho\sqrt{2\pi a^* t}}\ e^{-\frac{d^2}{4a^* t}} \qquad (12)$$

By differentiating Equation (12) with respect to t, and setting $\frac{\partial U}{\partial t}$ equal to zero, the time at which the temperature, U, is a maximum at the distance d, is found to be:

$$t_{max} = \frac{d^2}{2a^*} \qquad (13)$$

Substituting for d , in Equation (8), yields

$$U_{max}\Big|_d = \frac{Q_F}{c\ \rho\sqrt{4\pi a^* t_{max}}}\ e^{1/2} \qquad (14)$$

or

$$Q_F = \sqrt{4\pi 2 c \rho e t_{max}} \cdot U_{max}\Big|_d \qquad (15)$$

By determining the maximum temperature U_{max} at a known distance, d, and using Equation (15), the quantity of heat generated per unit crack length can be calculated.

III. DESIGN OF THE EXPERIMENT

3.1 Specimen and Test Frame

The material used in all tests, Plexiglas II, (polymethyl methacrylate) was chosen for several reasons:

1. It is a quasi-brittle material, behaving in fracture much like high strength steel and aluminum alloys, but fracturing at stress levels well below those of the alloys. This quality greatly reduces the size of the required loading facility and simplifies the design of a loading fixture.

2. It is a relatively isotropic material with little thickness effect on the fracture.

3. Plexiglas is a dielectric, hence the problem of insulating the velocity meter current paths is eliminated and the small thermal wave velocity assumption is satisfied. In addition, this very small wave velocity eliminates the need for a very high response electronic recording device.

The design of the specimen and test frame was the outgrowth of a previous investigation. Since the velocity data and experimental procedure is peculiar to the particular model, the basis of this design will be briefly discussed.

The test frame and specimen were designed as a unit,

hence the features of each are very much related to the other. An exploded view of the specimen-frame assembly is given in Figure 2. The test section itself is a 1/8 inch thick sheet of plexiglas, chosen to provide low working loads and thereby more nearly simulating the final fixed boundary conditions of the frame. All parts of the frame (except the plexiglas spacer plates) are 1/4 inch hot rolled, low carbon steel.

The specimen dimensions, given in Figure 3, which correspond to the dimensions of the frame, were chosen to satisfy the previously described boundary conditions. The values; b = 16 and h = 4, were chosen to provide a reasonably large (test) section over which quasi-static conditions could be maintained. To simplify the clamping procedure, the fixture was designed to load and clamp the specimen at the same points.

To distribute the load more evenly, "load spreader" strips (2"W x 16"L x 1/4"T) were attached to the specimen, with solvent, such that the inside edges were two inches from the centerline of the test plate thereby retaining the value; h = 4 inches. The specimen alignment within the frame and the clamping force, for both loading and clamping, was provided by Allenhead capscrews. (1/2"D x 2 1/4" in position A, 3/8"D x 2 1/2" in position B, and 5/8"D x 1 1/2" in position C). The upper and lower portions of the test frame were assembled with 3/8"D x 1 1/2" socket head capscrews.

hence the features of each are very much related to the other. An exploded view of the specimen-frame assembly is given in Figure 2. The test section itself is a 1/8 inch thick sheet of plexiglas, chosen to provide low working loads and thereby more nearly simulating the final fixed boundary conditions of the frame. All parts of the frame (except the plexiglas spacer plates) are 1/4 inch hot rolled, low carbon steel.

The specimen dimensions, given in Figure 3, which correspond to the dimensions of the frame, were chosen to satisfy the previously described boundary conditions. The values; b = 16 and h = 4, were chosen to provide a reasonably large (test) section over which quasi-static conditions could be maintained. To simplify the clamping procedure, the fixture was designed to load and clamp the specimen at the same points.

To distribute the load more evenly, "load spreader" strips (2"W x 16"L x 1/4"T) were attached to the specimen, with solvent, such that the inside edges were two inches from the centerline of the test plate thereby retaining the value; h = 4 inches. The specimen alignment within the frame and the clamping force, for both loading and clamping, was provided by Allenhead capscrews. (1/2"D x 2 1/4" in position A, 3/8"D x 2 1/2" in position B, and 5/8"D x 1 1/2" in position C). The upper and lower portions of the test frame were assembled with 3/8"D x 1 1/2" socket head capscrews.

The test load was applied to the upper and lower frame assemblies through 7/8"D pins, placed in the large holes labeled E (Figure 2), which were, in turn, attached to the test machine via cables. The load was transferred from the frame to the specimen by the friction between the frame grips and the load spreader strips. The normal force at the grips was controled by regulating the torque on bolts, A and C. The friction factor was increased, over the nominal value between steel and plexiglas, by roughing the faces of the frame grips with a center punch and hammer.

The reinforcing plates were clamped to the upper portion of the test frame during the loading of the specimen. After loading the specimen to the test conditions, the reinforcing plates were clamped to the low portion by tightening bolts, B, to a predetermined torque level. Thus secured, the frame satisfied the fixed boundary condition;

$$h + \Delta h = \text{constant (during fracture)}, \text{ since}$$

at the load levels used, the deflection of the steel reinforcing plates is nearly zero relative to the deflection of the specimen.

The crack was initiated at the left edge of the specimen (Figure 3) from the arm and hole arrangement. This section provided an area of nominal stress concentration at the "edge" of the specimen, making it possible to propagate a natural

crack into the test plate when required. A small saw cut was placed in the specimen at the right of the "starter hole" to accommodate a wedge, which was tapped lightly to initiate the crack.

3.2 Crack Velocity Measurement

The design goals for velocity measurement were two. First, to verify that the model provided constant crack velocity in the 8 inch test section for the entire loading range. Second, to determine the magnitude of the velocity (or speed), as a function of the gross stress.

The approach taken for this measurement was the use of a velocity meter (or gage) as described by Erdogan [16] and others [3,7,8]. Current paths to be severed by the passing crack were placed on the specimen perpendicular to the predicted crack path at known intervals. By connecting this switching arrangement to a suitable electrical circuit, and, in turn, to an oscilloscope, it was possible to measure the time between switchings and consequently the average crack velocity between switches. This method was relatively inexpensive, reliable and well suited to the test frame.

Having chosen the basic method by which the velocity was to be measured, the problem became one of finding an acceptable circuit arrangement. An oscilloscope, fitted with a Polaroid camera, was available, providing a versatile recording device. Two simple, bridge type circuits, which incorporate the switching mechanism and which were tried as possible solutions are diagramed in Figure 4. Examination of these circuits reveals the general approach of investigators to this circuitry problem.

When the crack severs one of the current paths, the voltage across the circuit output (oscilloscope input) terminals is changed, causing a change in the vertical position of the scope trace. The scope sweep rate is set at a value which is hopefully compatible with the speed of fracture. That is, for the greatest accuracy, the test section length must be closely represented by the full width of the scope grid. The time, and, in turn, the velocity, is determined by measuring the distance between voltage changes for a trace of known speed.

Circuit 1, (Figure 4a) provides a 1.5 volt step input, alternating plus and minus, with the successive breaking of current paths. The ideal result would be a square wave like that shown in Figure 4b. Circuit 2, (Figure 4c) provides a step voltage increase followed by an exponential decay to the zero value. The rate of decay is governed by the size of the capacitor. Thus the trace consists of a series of peaks marking the breaking of each current path, as illustrated in Figure 4d.

There are several obvious shortcomings to this approach to the measurement of time. First, the accuracy of the data is very dependent on one's ability to guess or calculate the crack velocity. It is further limited by the resolution of the trace speed on the oscilloscope. With patience and perseverance, one can measure the velocity, as many have, but the accuracy and repeatability are not as good as one might desire. In fact, both of the circuits, illustrated in Figure 4, were

tried and found unsatisfactory for this work. Since the problem was one of measuring the times of a sequence of events, the ideal solution was a device, with its own time standard, that could be turned on and off by the existing switching arrangement. With such a device, the time could be determined directly, eliminating the problem of matching the measuring device to the event time, before each test. Such a device was designed and developed under the direction of Dr. Barrett*, and will be called, hereafter, the "electronic timer".

This electronic timer is capable of measuring the duration of each of a series of nine events in the range, 32 to 1024μ sec., with a resolution of $\pm$ 1μ sec., or in the range, 110 to 10240μ sec., $\pm$ 10μ sec. The output is a binary number which is reproduced on an oscilloscope screen. An example of the output for an actual velocity test is presented in Figure 5. Each horizontal trace, except the top one, represents the time for one event. The brighter segments are read as ones (1's) and the darker segments are read as zeros (0's). For example, the second trace (from the top) is read 0000110111 which is the binary number corresponding to 55. The duration of this event is then 56μ sec., since 1μ sec. must be added to the recorded time to correct for a count missed during an internal switching operation**.

---

* William A. Barrett, Associate Professor of Electrical Engineering, Lehigh University.

** A detailed explanation of the need for this correction is offered in Appendix C.

The electronic timer contains two crystals (100 kc and 1000 kc) which serve as time standards and its own voltage regulator. Consequently, an oscilloscope and a single D.C. voltage source are the only external electronic equipment necessary. Dr. Barrett's explanation of the design theory and detailed electronic operation of the timer, along with a detailed circuit diagram is presented in Appendix C.

The cost of the electronic timer, excluding labor and design costs, was approximately $300.00 which includes a $90.00 low voltage power supply. For the sake of comparison, a single event, commercial, micro second timer will normally cost more than $1000.00.

3.3 Heat Generation Measurement

The goal of this design was the measurement of the surface temperature of the specimen, as a function of the time after fracture, at a known distance from the crack face. This had to be accomplished accurately and reliably and above all, without effecting the established experimental conditions.

The specific problem characteristics which effected the design were:

1. The magnitude of the temperature gradient expected for plexiglas was of the order of 1°F. This was a result of the low stress levels required to support fracture. For metals, the expected gradient would be from one to two orders of magnitude higher.

2. The velocity of the thermal wave was expected to be quite low since plexiglas is a dielectric.

3. For the same reason, the values of the temperature and time to reach a maximum were very dependent on the distance from the crack face. For example, using the expression, Equation (13), for t_{max} developed under analytical considerations the following values were calculated:

When d = 1 cm; t_{max} = 4.12 sec.

When d = 1 cm; t_{max} = 412 sec.

4. Thermocouple conduction could effect the experimental conditions, since the conductivity of the sensor would, most likely, be much greater than that of plexiglas. Consequently, the sensor would act as a heat sink.

5. The environmental effects such as natural convection were of unknown magnitude.

The following guide lines were developedonthe basis of the above characteristics. The sensor had to be small and yet have a large signal per degree output ratio. High gain amplification was required but high response was not essential. The recording device was to have its own time base and be compatible with both the sensor and amplifier. A method for positioning the sensor was needed which would permit sensible calibration and reliable placement. An excellent calibration technique, to include environmental effects was required. Above all, the total cost was to be minimal.

An exposed junction Chromel-Constantan thermocouple probe, 1/16"D, using 0.002 inch diameter wire was the selected sensor. It was relatively inexpensive, small (bead diameter was 0.006 inch), rugged (probe configuration protects junction and leads), easily positioned and had the largest output per degree of any thermocouple, (33.65μV/°F).

Two amplifiers were selected; a X10,000 low level preamplifier was part of the recording system and a X1,000 pre-

amplifier was designed from standard Fairchild Microamp.® circuitry. The recording system was a Sanborn (Hewlett Packard) 850 system with a four-channel recorder, two low level preamplifiers and two carrier-preamplifiers. The fixture shown in Figure 6 was designed to hold the thermocouple probe, and identify its position by using a micrometer barrel.

Time did not allow for the completion of this apparatus or the development of a calibration technique. However, the design is felt to be sound and to warrant further investigation.

IV. TEST PROCEDURE

4.1 Specimen Preparation

To eliminate unnecessary inconsistencies in the experimental results, all of the specimens were made at one time and all were cut with the same orientation from a commercially cast, 1/8" thick, sheet of Plexiglas II. The inside edges of the load spreaders were machined square, and aligned two inches above and below, the centerline of the plate. The starter system, including the hole but not the saw cut, was included in the original preparation.

The current paths were placed on the specimens just before testing; their configuration depending on the type of test being conducted. After the saw cut had been made, the specimen was wiped clean with a clean-dry soft cloth, and the current paths were prepared. For the standard path configuration (Figure 7a) marks were lightly scribed on the specimens at one inch increments, beginning three inches from the starting edge. Using 3/4 inch masking tape, lines (approximately 1/32 inch wide) were laid out on the marks, perpendicular to the predicted crack path. Two and one half inch long current paths were then formed by brushing silver paint (a suspension of silver alloy in butyl acetate) onto the plate. The masking tape was removed as soon as the paint appeared dry (approximately 2 minutes after application).

Two contact strips, (Figure 8), were placed on the specimen as shown in Figure 7 using two strips of double sticking cellophane tape. The current paths were then completed by extending the 2 1/2 inch lines up the copper contact ramps, with the silver paint, (Figure 8). The acceleration and velocity vs. crack length configurations required a more elaborate system of connecting lines (Figure 7b, 7c), since it was not practical to make new contact strips for these cases.

4.2 Test Frame Assembly

The specimen was aligned in the test frame by the insertion of all of the capscrews (bolts) into their proper positions. All of the bolts, except the inside four in position B (Figure 2) were wrench tightened. Before moving the frame to the test machine, the six bolts in position A were torqued down with 45-foot-pounds, clamping the reinforcing plates to the upper part of the test frame and specimen. The assembly was then hung in the test machine, with cables, as previously described, and the connecting cable for the electronic timer was secured to prevent the contact strips from being accidently dislodged. Finally, the bolts in position C were torqued down with 45-foot-pounds and the two bottom, outside bolts (position B) were loosened. In this state, bolts A and C with 45-foot-pounds torque and bolts B loose, the specimen was ready for loading.

4.3 Testing

From this point on, the order of operations followed the checklist given in Appendix D. Due to the number of operations which had to be performed in sequence, these lists proved to be indispensable. Generally, the test frame was rechecked and the instrumentation was inspected, tested and adjusted before loading the specimen. Continuity, for this test, was obtained when the resistance of each of the current paths and connecting wires was less than 30 ohms or when the voltage across the times input terminals was less than + 0.1 volt. The sequence under CLOCK (Appendix D) was the procedure followed to produce a test pattern on the oscilloscope screen, permitting positioning and trace adjustments before each test.

To absorb most of the cable slack, the specimen was preloaded with 100 pounds, and the test frame was aligned for plumb with a 6 inch plumb rule. The load was then applied at a prescribed rate and maintained at the particular test load while the reinforcing plates were clamped into place with 35 foot-pounds torque on the bolts in position B. The instrumentation was again checked. (The total time for the tightening and checking operations was less than five minutes). A natural crack was then propagated through the specimen by tapping a wedge placed directly in the saw cut. The timer output was removed from the scope camera after the grid was added to the picture and the continuity was again checked to deter-

mine which paths had been severed. A severed path was indicated by a voltage of + 1.4 volts or more across the timer input terminals.

As mentioned earlier, no temperature measurements were made in the course of this investigation. However, it is expected the "hold time" before crack initiation will be increased to allow time to position the probe, zero the recorder and conduct additional checks as made in the present procedure.

V. DISCUSSION OF DESIGN AND OPERATION

Although the constant velocity across the model's test section was evidence that the design conditions had been satisfied, several shortcomings of the frame and specimen assembly bear mentioning:

1. The process of assembling and disassembling the test frame for every test was very tedious, requiring more than an hour per test. The design and use of an assembly table simplified the task somewhat, but did not eliminate any work.

2. The performance of the fixture proved somewhat temperamental. The addition of load spreader strips on the specimens and the roughening of the grips along with attention to the details of a carefully engineered experimental procedure (see Appendix D) greatly improved the frequency of acceptable tests.

3. The fractures consistently propagated in the upper half of the specimen test section as a result of the specimen-test frame clamping design. The absence of normal pressure on the outside portions of the lower load spreaders, caused by, and in addition to, the unsymmetrical arrangement of the bolt holes is believed to be the cause of this behavior.

The electronic timer performed its function as designed, although, in several cases, its limitations were exceeded. The lower limit on the duration of an event is approximately 32μ sec. [11μ sec. were required to shift the stored information out of the timer to the oscilloscope (1μ sec. per binary digit plus 1μ sec. for switching) plus the oscilloscope had an internal lock out which prevented a new trace without 20μ sec. delay after the completion of the preceding trace]. When the event times were less than 32μ sec. a trace was lost, and only every other event time was recorded. This is the reason for the missing values in Table 8.

Dr. Barrett points out, in Appendix C, that the time resolution is limited at 0.5μ sec. due to the 2 megacycle frequency limitations of the integrated circuits. If more resolution is desired, more expensive logic units, with a 20 megacycle limit, may be purchased.

The double gate arrangement in the INP stages, labeled INA 1,..., was added after the time required to break a current path was found to be too long. The logic elements demand a switching time (or fall time) less than 50 nanoseconds when changing from one logic state to the other. The INA arrangement increases the fall rate of the switching signal to within the 50 nanosecond limit.

The final alteration was made to provide the test pattern mentioned in Chapter IV. By connecting the oscilloscope calibrator circuit to the input terminal of INP 1, events were produced at a rate of one per millisecond. This produced a pattern on the oscilloscope screen with the same intensity and position as the actual test data. The "switch clear" switch set the logic units in the INP stages and when closed allowed continuous switching of the first stage. The "shift clear" switch cleared the event register, EC1, EC2,..., in order to set the vertical position of the trace at the top of the screen. Hence, to assure proper timer operation, it was essential that these two switches be closed and then opened, just prior to opening the camera shutter and initiating the crack.

VI. DISCUSSION OF TEST RESULTS

Eleven successful tests, at stress levels ranging from 1000 to 4500 psi., were conducted using the electronic timer. All tests were made at room temperature (75°F) with a loading rate of 10 pounds per second. The humidity was not considered. The detailed data is presented in Tables 2 to 12.

All of the cracks ran in the upper half of the specimen, and branching occurred in only one case, 4500 psi. Slight "surface runners" were noticeable at lower stress levels (3000 and 3500 psi.). The roughness of the fracture surface increased with velocity in agreement with observations by Cotterell [7]. The fixture consistently produced reasonably straight fractures at the 2500 - 3500 psi. stress level. The crack ran above the test section at 1000 psi., branched at 4500 psi., while the 1500 - 2000 psi. range was characterized by unpredictable paths. Sketches of all crack paths are included in Tables 2 to 12.

The test section quasi-static velocity increased with the gross stress and reached a maximum of more than 2180 ft./sec. before branching occurred. This value is in agreement with Cotterell's [7] experimentally determined value of 2200 ft./sec. and the theoretical value of Dulaney and Brance, 2330 ft./sec.

The reproducibility of data was excellent in all but one case (2500 psi. - Table 9) where a thickness variation of

- 0.020 inches over the cross section (and from the normal specimen thickness) was measured. The constant (average of the recorded values) velocities and the corresponding values of gross stress, σ, stress intensity factor, K, and crack extension force, G, are given in Table 1. The plots of K as a function of velocity, V_c, is given in Figure 11, while G as a function of V_c is plotted in Figure 12.

Additional tests were run to examine the acceleration of the crack from the starting edge to the quasi-static value, and also to determine the model's overall velocity variation with crack length. Since the width of the test section was reduced for these tests (see Figure 7b and Figure 7c), 2500 psi. was chosen as the stress level, to insure a predictable crack path. The results of the acceleration test are tabulated in Table 8 and plotted in Figure 13 while those for the velocity variation are tabulated and plotted in Table 9 and Figure 14, respectively.

All time values were resolved to plus or minus one microsecond. In terms of percent error this represented a range, depending on the crack velocity, of from $\pm$ 0.81% to $\pm$ 2.5% for the standard section velocity test. The maximum error for any test was that $\pm$ 3.6% error for the acceleration test caused by the use of 1/2 inch wide segments. The maximum error possible before traces were missed was approximately $\pm$ 3.0%. The crystal was calibrated at 999.835 kc's at room temperature.

Additional errors may have been caused by the varying thicknesses of the current paths (< 0.8%) and the measurement of the segment widths (< 0.8%). The thickness error was absorbed for the most part by the $\pm$ 1μ sec. tolerance as was the error due to the measurement of the segment widths.

A thickness variation of up to - 0.007 in. from the nominal value of 0.125 in. was observed on all specimens. For convenience of calculation, the nominal value was retained as exact.

VII. CONCLUSIONS AND RECOMMENDATIONS

The velocity behavior followed the predicted pattern for the fixed boundary model and the magnitude was found to approach the 2200 ft./sec. value, experimentally determined by Cotterell [7]. The theoretical value for the terminal velocity predicted by Dulaney and Brace of 7.1×10^4 cm./sec. or 2330 ft./sec. (using Roberts' and Well's value $V_T/(E/\rho)^{1/2}$ = 0.38) was also in the range of the 2180 ft./sec. velocity measured during branching, at 4500 psi. However, more acceleration measurements at the higher stress levels (to determine the velocity just prior to branching) are necessary before making any statements about that region and the actual terminal value. The feasibility of such a study with the designed timing device has been shown.

As the stress level was increased, the value of the constant section velocity increased, but by a smaller amount with each successive increase. This behavior, as represented by the K vs. V_c and G vs. V_c curves, agreed with that predicted by Lucas [17], although no curve fit was attempted to determine the precise correlation. For such a correlation, more data will be required at both the upper and lower stress levels.

It is highly recommended that a new test frame and specimen be developed before the heat generation measurement and experimental analysis of the velocity-crack length relation

across the model are attempted. The temperamental nature of the present specimen-frame arrangement and the eratic nature of the crack path will prove detrimental to such studies. In addition, the experimental time and effort require to get acceptable data is prohibitive to any extensive study.

An alteration of the electronic timer might also be investigated. By using a dual trace oscilloscope and splitting the timer output so that the time intervals are alternated from one oscilloscope trace to the other, the timer range will be increased to a lower limit of approximately 11μ sec.

VIII. TABLES

Table 1.

Constant Section Velocity Data

P (lb)	σ (psi)	K (lb/in$^{3/2}$)	G (lb/in)	V_c (ft/sec)
2000	1000	1414	4.45	720
3000	1500	2120	10.0	870
3000	1500	2120	10.0	890
3000	1500	2120	10.0	832
4000	2000	2830	17.8	1202
5000	2500	3540	27.9	1520
5000	2500	3540	27.9	1515
5000	2500	3540	27.9	1690
6000	3000	4240	40.0	1810
7000	3500	4950	54.4	1975
9000	4500	6360	90.0	2180

Note: K_c was experimentally determined for one plate with a central crack, in simple tension, where 2a = 1 in. and 2b = 16 in. At the onset of rapid fracture:

$$a = 0.57 \text{ in.}$$

$$\sigma = 770 \text{ psi.}$$

hence, using Eq.(4),

$$K_c = 1030 \text{ lb/in.}^{3/2}$$

and, from Eq.(7),

$$G_c = 2.36 \text{ lb/in.}$$

Table 2.

Load Level: 2000 lb.

Stress Level: 1000 lb./in.^{2}

Loading Rate: 10 lb./sec.

Timer Range: 1000 kc.

Comments: Paths 1, 2, and 5 not severed.

LOCATION NUMBER	CRACK LENGTH (in.-in.)	TIME (μsec.)	SEGMENT WIDTH (in.)	VELOCITY (ft./sec.)
9	3 - 4	108	1.031	795
8	4 - 5	117	1.031	734
7	5 - 6	120	1.023	710
6	6 - 7	144	1.016	587
5	7 - 8	634	-----	------
4	8 - 9	306	-----	------
3	9 - 10	---	-----	------
2	10 - 11	---	-----	------
1	11 - 12	---	-----	------

Crack Path in Test Section: Half Scale.

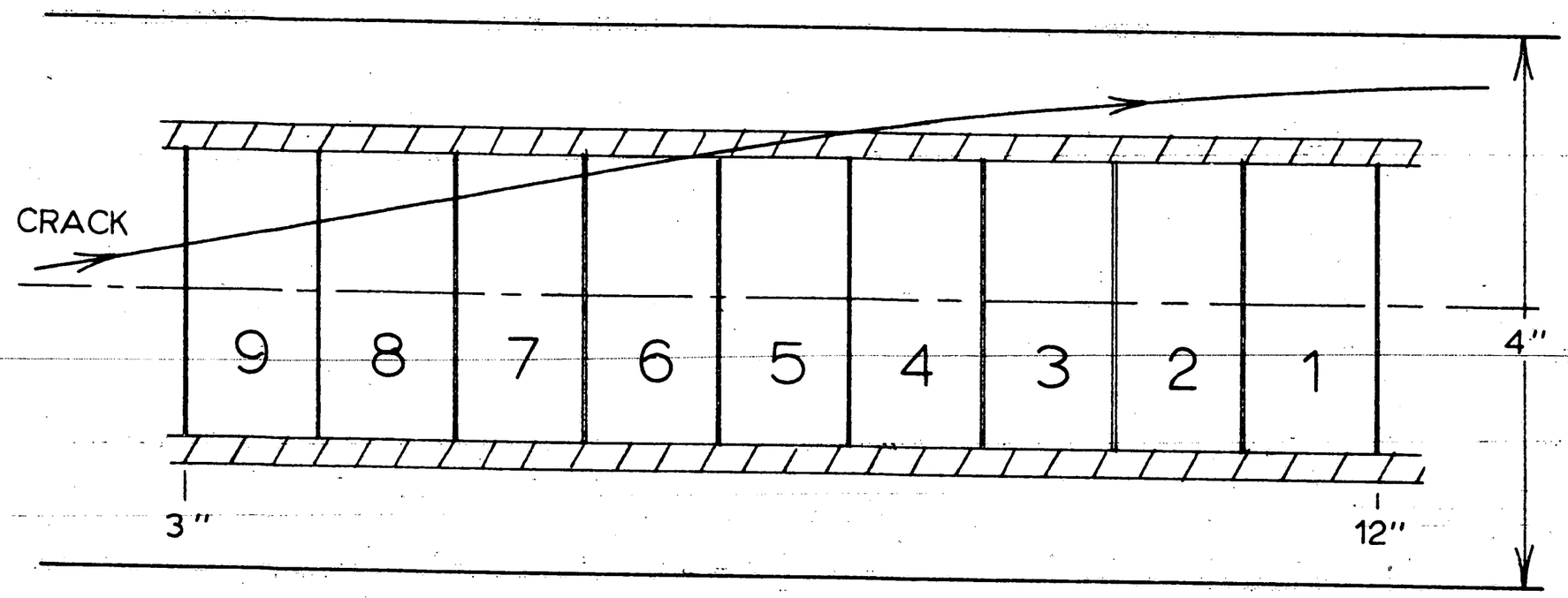

Note: When the crack severed a current path in the cross-hatched area, the time was recorded but the distance could not be measured.

Table 3.

Load Level: 3000 lb.
Stress Level: 1500 lb./in.^{2}
Loading Rate: 10 lb./sec.
Timer Range: 100 kc.
Comments:

LOCATION NUMBER	CRACK LENGTH (in.-in.)	TIME (μsec.)	SEGMENT WIDTH (in.)	VELOCITY (ft./sec.)
9	3 - 4	---	1.031	-------
8	4 - 5	90	0.969	897
7	5 - 6	---	1.000	-------
6	6 - 7	90	1.000	926
5	7 - 8	---	1.000	-------
4	8 - 9	90	1.000	926
3	9 - 10	---	1.000	-------
2	10 - 11	90	0.984	910
1	11 - 12	---	1.000	-------

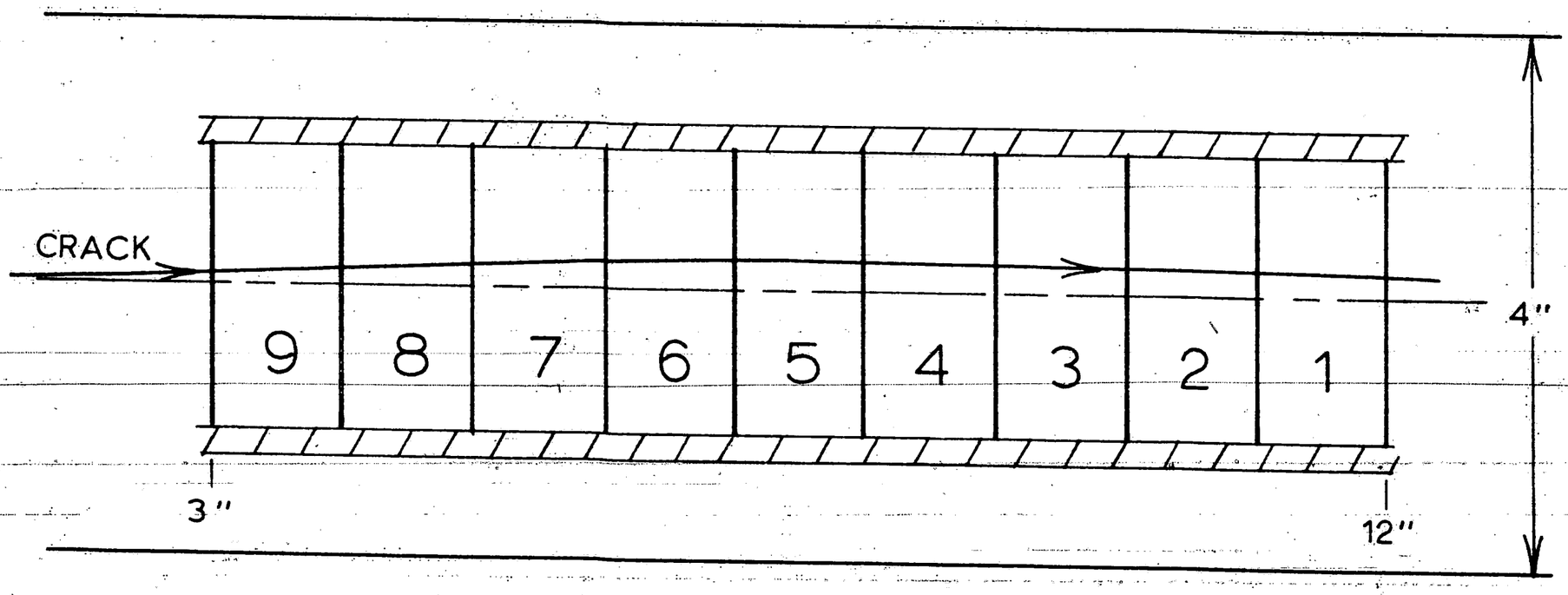

Table 4.

Load Level: 3000 lb.

Stress Level: 1500 lb./in.^{2}

Loading Rate: 10 lb./sec.

Timer Range: 1000 kc.

Comments: Crack ran out of test section in Location 5.

LOCATION NUMBER	CRACK LENGTH (in.-in.)	TIME (μsec.)	SEGMENT WIDTH (in.)	VELOCITY (ft./sec.)
9	3 - 4	92	1.015	934
8	4 - 5	97	1.015	875
7	5 - 6	96	1.023	890
6	6 - 7	102	1.047	855
5	7 - 8	111	-----	-------
4	8 - 9	---	-----	-------
3	9 - 10	---	-----	-------
2	10 - 11	---	-----	-------
1	11 - 12	---	-----	-------

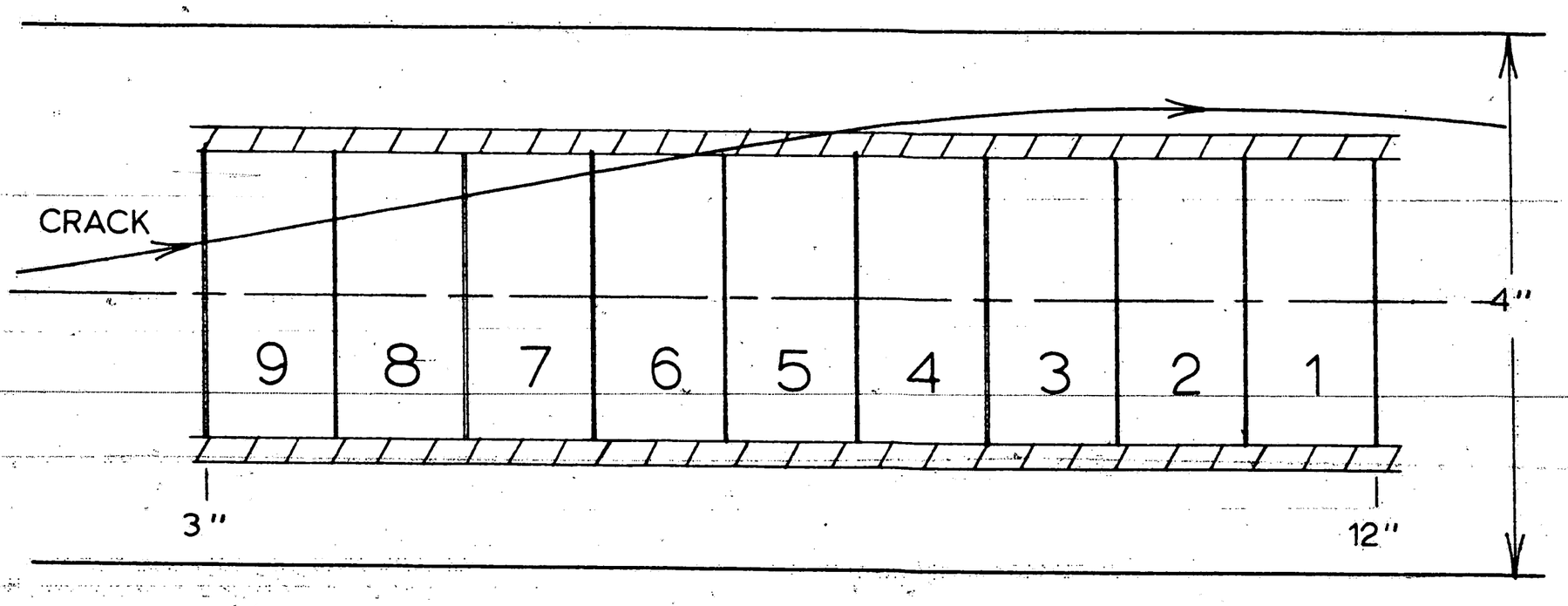

Table 5.

Load level: 3000 lb.

Stress Level: 1500lb./in.^{2}

Loading Rate: 10 lb./sec.

Timer Range: 1000 kc.

Comments:

LOCATION NUMBER	CRACK LENGTH (in.-in.)	TIME (μsec.)	SEGMENT WIDTH (in.)	VELOCITY (ft./sec.)
9	3 - 4	100	1.000	834
8	4 - 5	98	1.000	850
7	5 - 6	101	1.015	837
6	6 - 7	105	1.007	800
5	7 - 8	100	1.000	834
4	8 - 9	99	1.000	842
3	9 - 10	101	1.000	825
2	10 - 11	100	1.000	834
1	11 - 12	100	1.000	834

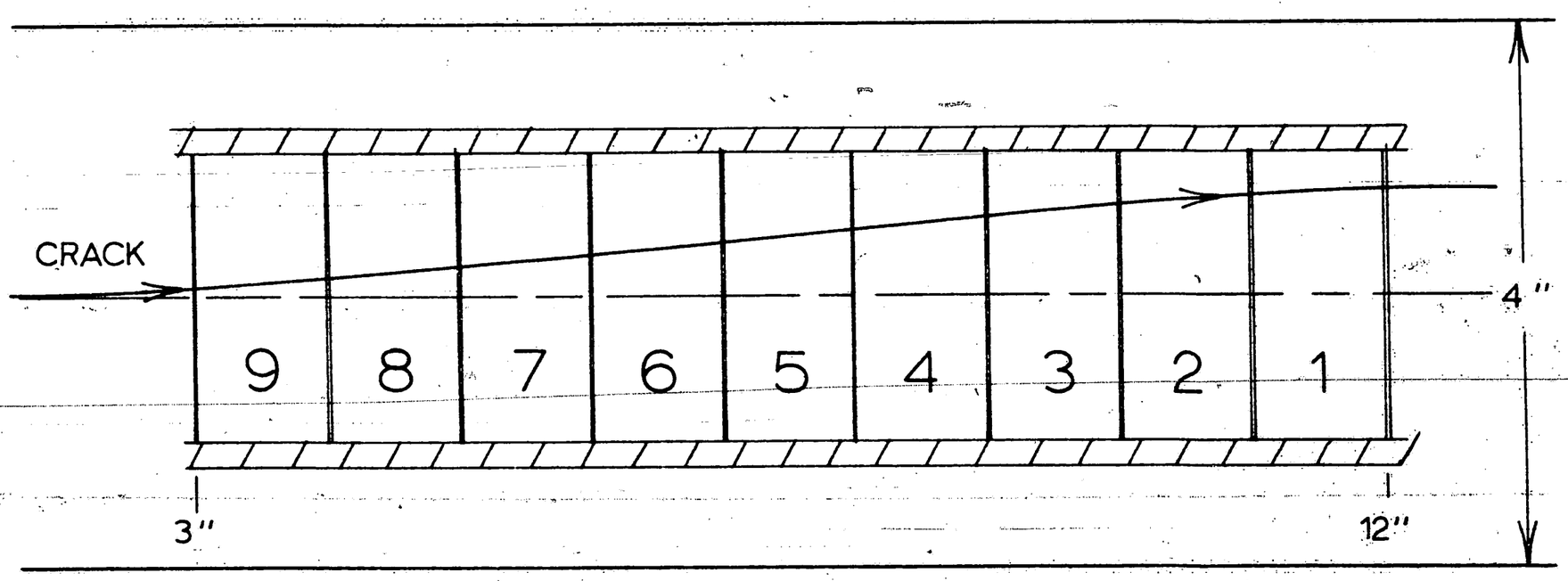

Table 6.

Load Level: 4000 lb.

Stress Level: 2000 lb./in.^{2}

Loading Rate: 10 lb./sec.

Timer Range: 1000 kc.

Comments: Crack ran out of test section in Location 6.

LOCATION NUMBER	CRACK LENGTH (in.-in.)	TIME (μsec.)	SEGMENT WIDTH (in.)	VELOCITY (ft./sec.)
9	3 - 4	74	1.031	1161
8	4 - 5	70	1.016	1208
7	5 - 6	68	1.007	1236
6	6 - 7	72	-----	-------
5	7 - 8	75	-----	-------
4	8 - 9	77	-----	-------
3	9 - 10	73	-----	-------
2	10 - 11	116	-----	-------
1	11 - 12	---	-----	-------

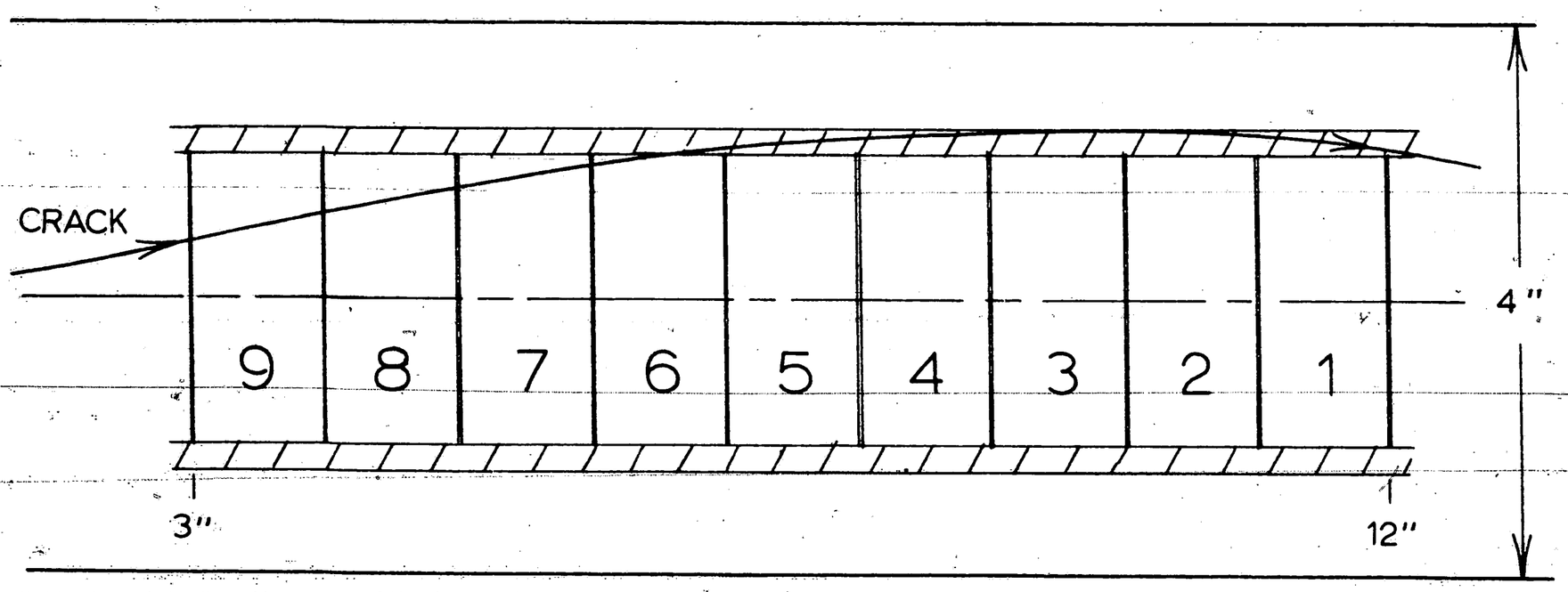

Table 7.

Load Level: 5000 lb.

Stress Level: 2500 lb./in.^{2}

Loading Rate: 10 lb./sec.

Timer Range: 1000 kc.

Comments:

LOCATION NUMBER	CRACK LENGTH (in.-in.)	TIME (μsec.)	SEGMENT WIDTH (in.)	VELOCITY (ft./sec.)
9	3 - 4	56	1.000	1490
8	4 - 5	55	1.000	1515
7	5 - 6	55	1.000	1515
6	6 - 7	53	0.984	1545
5	7 - 8	55	1.000	1515
4	8 - 9	54	1.000	1540
3	9 - 10	55	1.000	1515
2	10 - 11	55	1.016	1540
1	11 - 12	55	1.000	1515

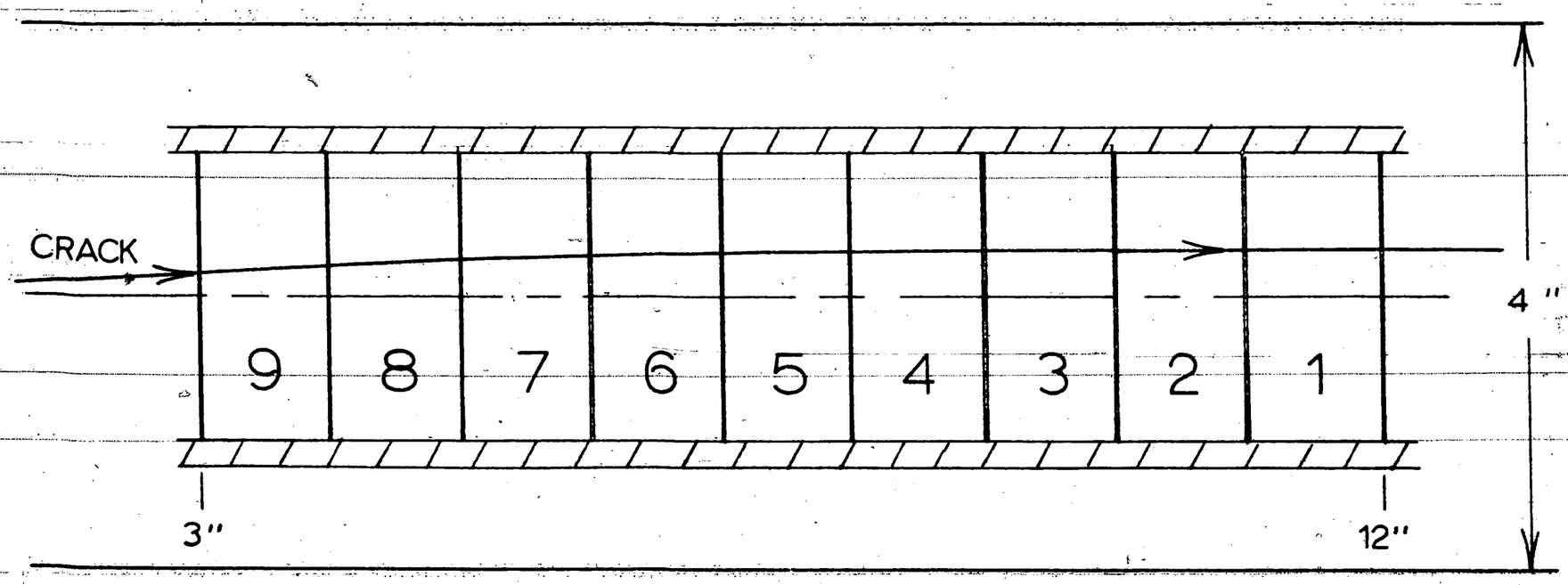

Table 8.

Load Level: 5000 lb.

Stress Level: 2500 lb./in.^{2}

Loading Rate: 10 lb./sec.

Timer Range: 1000 kc.

Comments: Acceleration Test.

LOCATION NUMBER	CRACK LENGTH (in.-in.)	TIME (μsec.)	SEGMENT WIDTH (in.)	VELOCITY (ft./sec.)
9	1/4-3/4	51	0.500	817
8	3/4-1 1/4	41	0.507	1030
7	1 1/4-1 3/4	---	0.507	-------
6	1 3/4-2 1/4	30	0.500	1390
5	2 1/4-2 3/4	---	0.507	-------
4	2 3/4-3 1/4	28	o.507	1510
3	3 1/4-3 3/4	---	0.515	-------
2	3 3/4-4 3/4	54	1.000	1540
1	4 3/4-5 3/4	56	1.000	1490

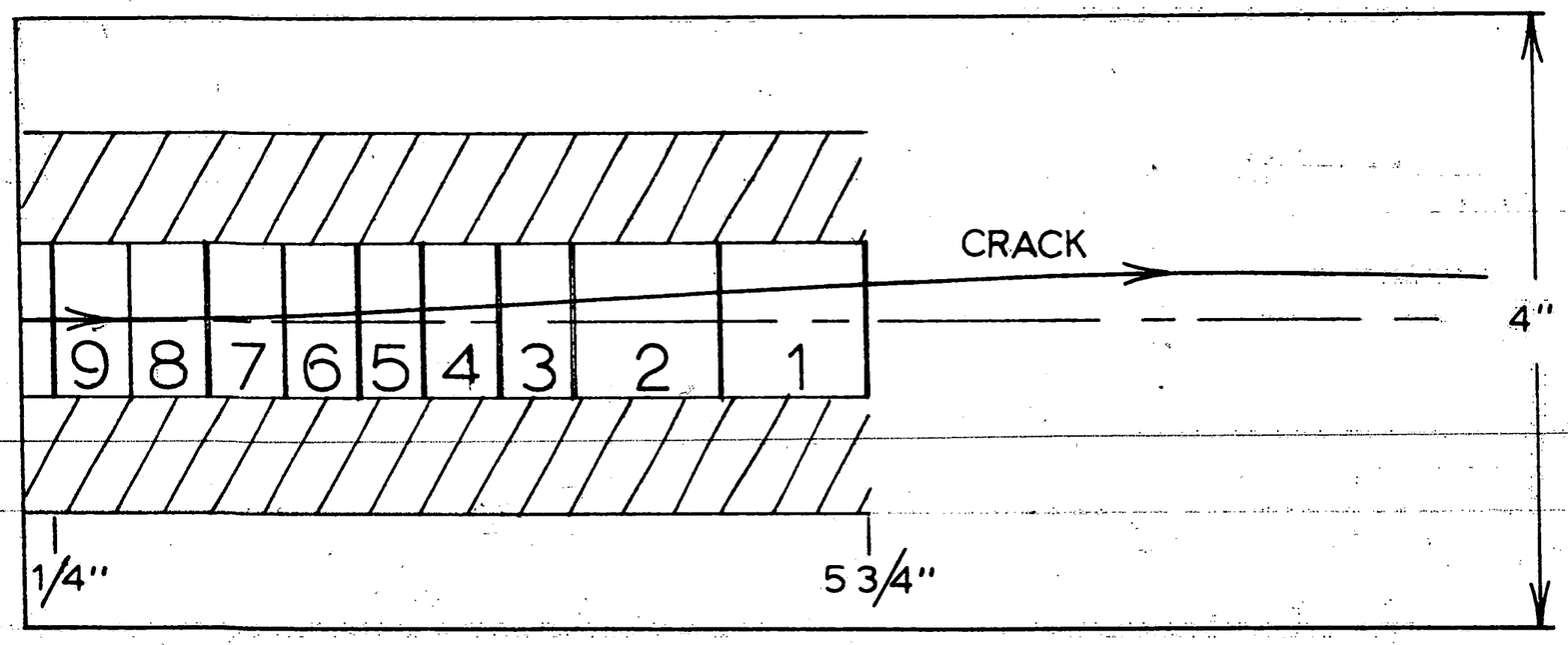

Table 9.

Load Level: 5000 lb.

Stress Level: 2500 lb./in.^{2}

Loading Rate: 10 lb./sec.

Timer Range: 1000 kc.

Comments: Velocity measured over entire model.
Crack ran out of test section at Location 5 and back in at Location 4.

LOCATION NUMBER	CRACK LENGTH (in.-in.)	TIME (μsec.)	SEGMENT WIDTH (in.)	VELOCITY (ft./sec.)
9	1/8 - 1	66	0.875	1105
8	1 - 2	50	1.000	1670
7	2 - 3	47	1.000	1770
6	3 - 4	47	1.000	1770
5	4 - 12	401	8.125	1690
4	12 - 13	---	-----	-------
3	13 - 14	119	0.937	1350
2	14 - 15		1.000	
1	15 - 16	67	0.875	1090

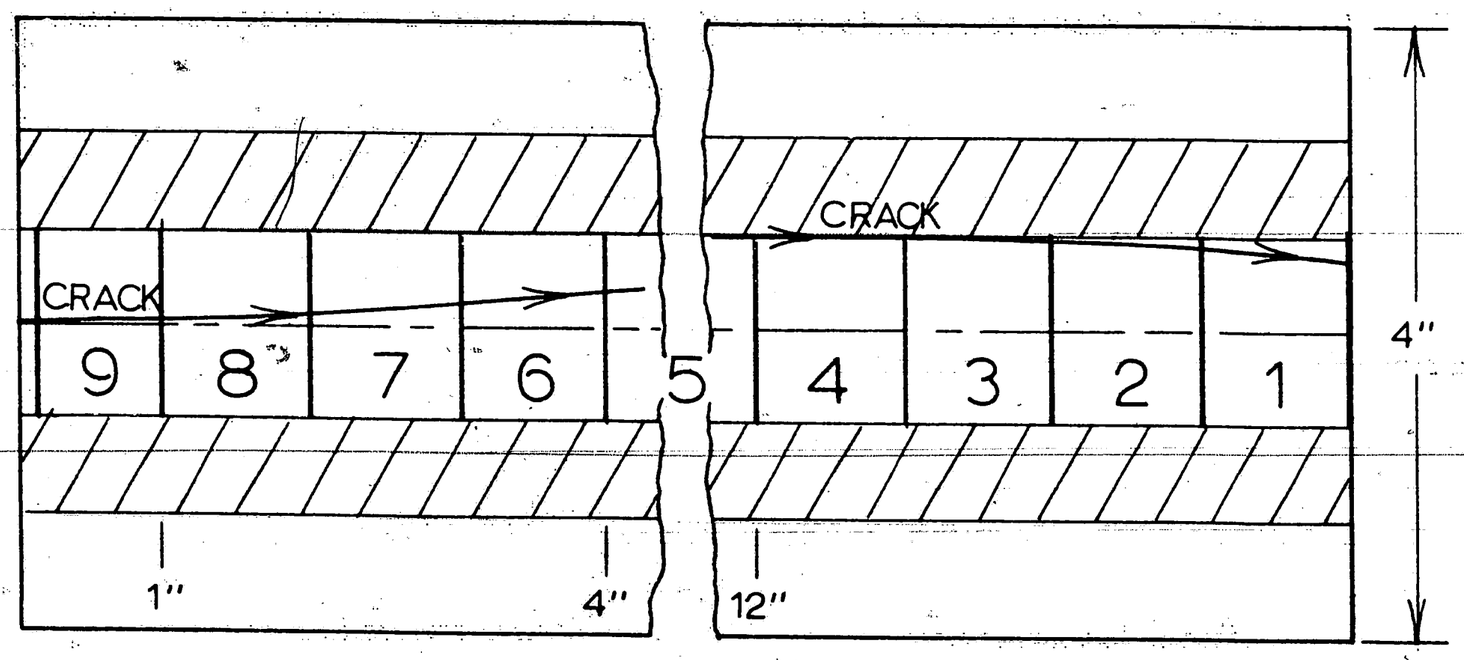

Table 10.

Load Level: 6000 lb.

Stress Level: 3000 lb./in.^{2}

Loading Rate: 10 lb./sec.

Timer Range: 1000 kc.

Comments:

LOCATION NUMBER	CRACK LENGTH (in.-in.)	TIME (μsec.)	SEGMENT WIDTH (in.)	VELOCITY (ft./sec.)
9	3 - 4	47	1.023	1815
8	4 - 5	45	1.000	1850
7	5 - 6	45	1.000	1850
6	6 - 7	46	1.000	1810
5	7 - 8	45	1.000	1850
4	8 - 9	46	1.000	1810
3	9 - 10	47	1.000	1771
2	10 - 11	47	1.007	1785
1	11 - 12	48	1.000	1737

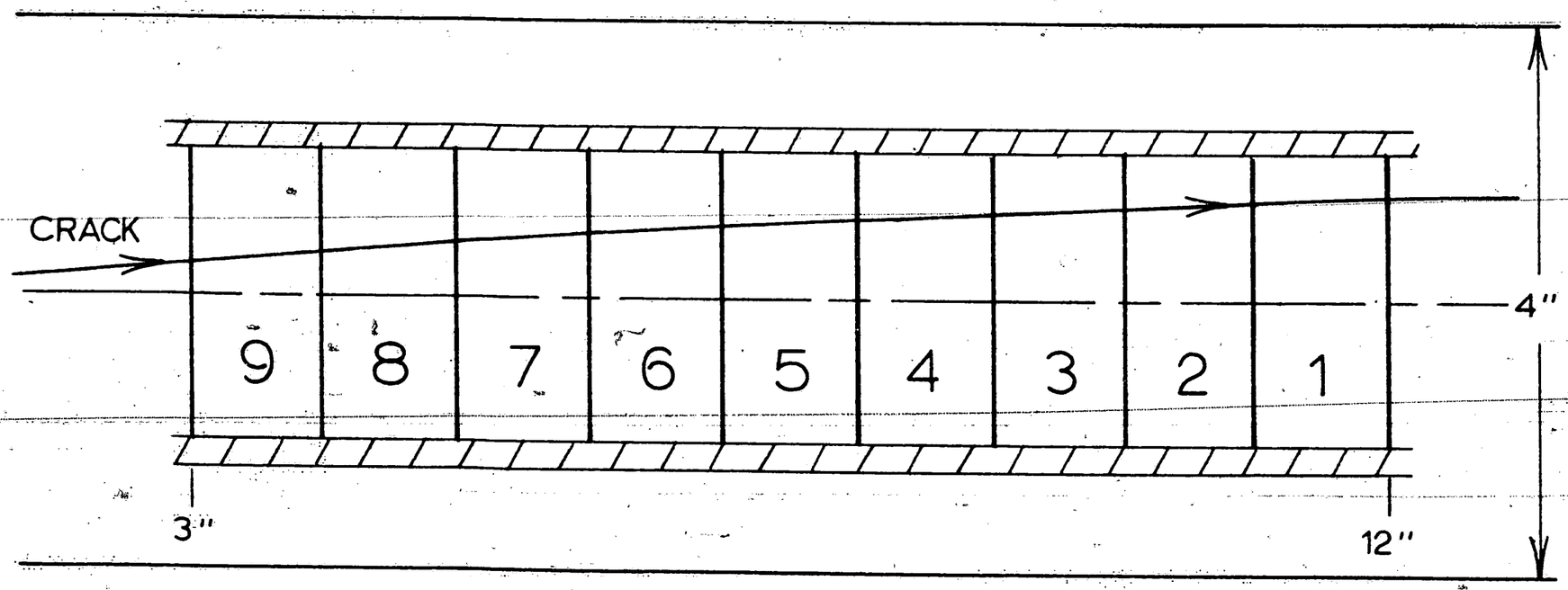

Table 11.

Load Level: 7000 lb.

Stress Level: 3500 lb./in.^{2}

Loading Rate: 10 lb./sec.

Timer Range: 1000 kc.

Comments:

LOCATION NUMBER	CRACK LENGTH (in.-in.)	TIME (μsec.)	SEGMENT WIDTH (in.)	VELOCITY (ft./sec.)
9	3 - 4	43	1.016	1970
8	4 - 5	43	1.000	1940
7	5 - 6	42	1.007	1995
6	6 - 7	42	1.000	1985
5	7 - 8	43	1.000	1940
4	8 - 9	43	1.000	1940
3	9 - 10	43	1.007	1950
2	10 - 11	41	1.000	2030
1	11 - 12	44	0.993	1890

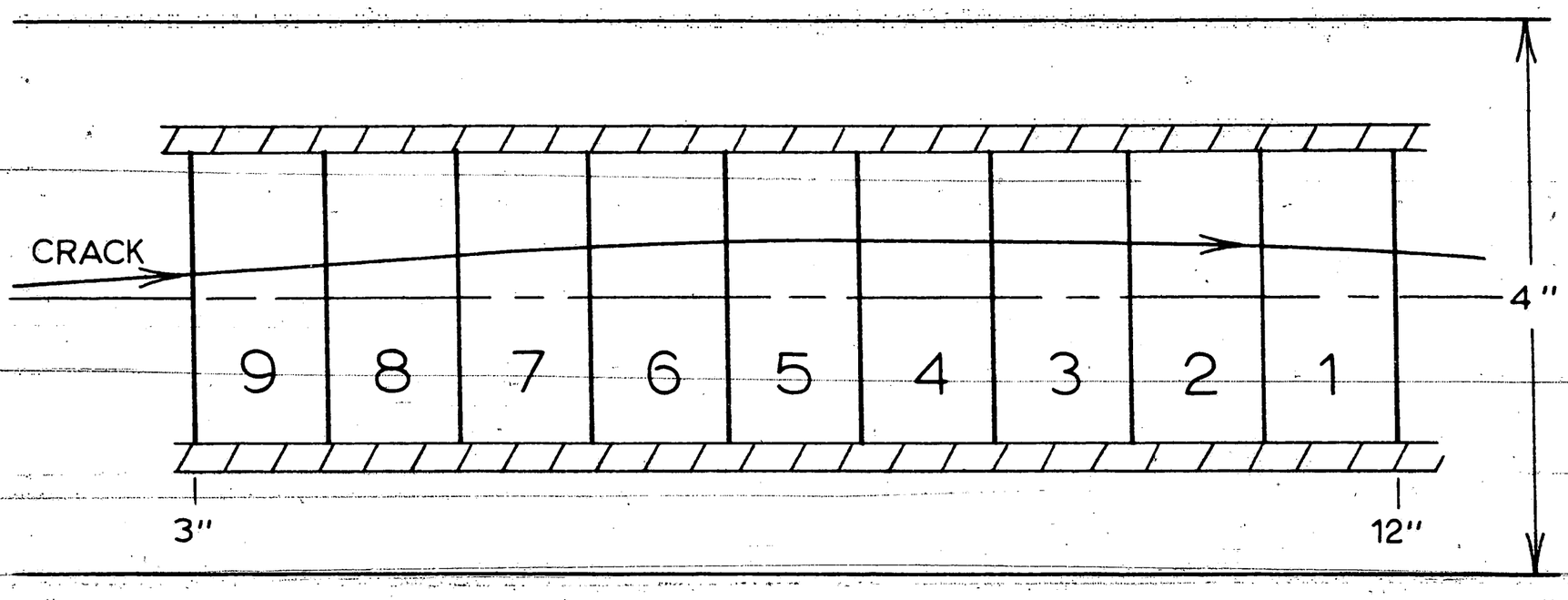

Table 12.

Load Level: 9000 lb.
Stress Level: 4500 lb./in.^{2}
Loading Rate: 10 lb./sec.
Timer Range: 1000 kc.
Comments: Branching occurred in Location 9.
Lead crack ran out of test section at Location 7.
Trailing crack at Location 3.

LOCATION NUMBER	CRACK LENGTH (in.-in.)	TIME (μsec.)	SEGMENT WIDTH (in.)	VELOCITY (ft./sec.)
9	3 - 4	40	1.047	2180
8	4 - 5	46	1.062	1925
7	5 - 6	45	1.031	1910
6	6 - 7	45	1.031	1910
5	7 - 8	46	1.031	1870
4	8 - 9	47	1.031	1830
3	9 - 10	---	-----	-------
2	10 - 11	---	-----	-------
1	11 - 12	---	-----	-------

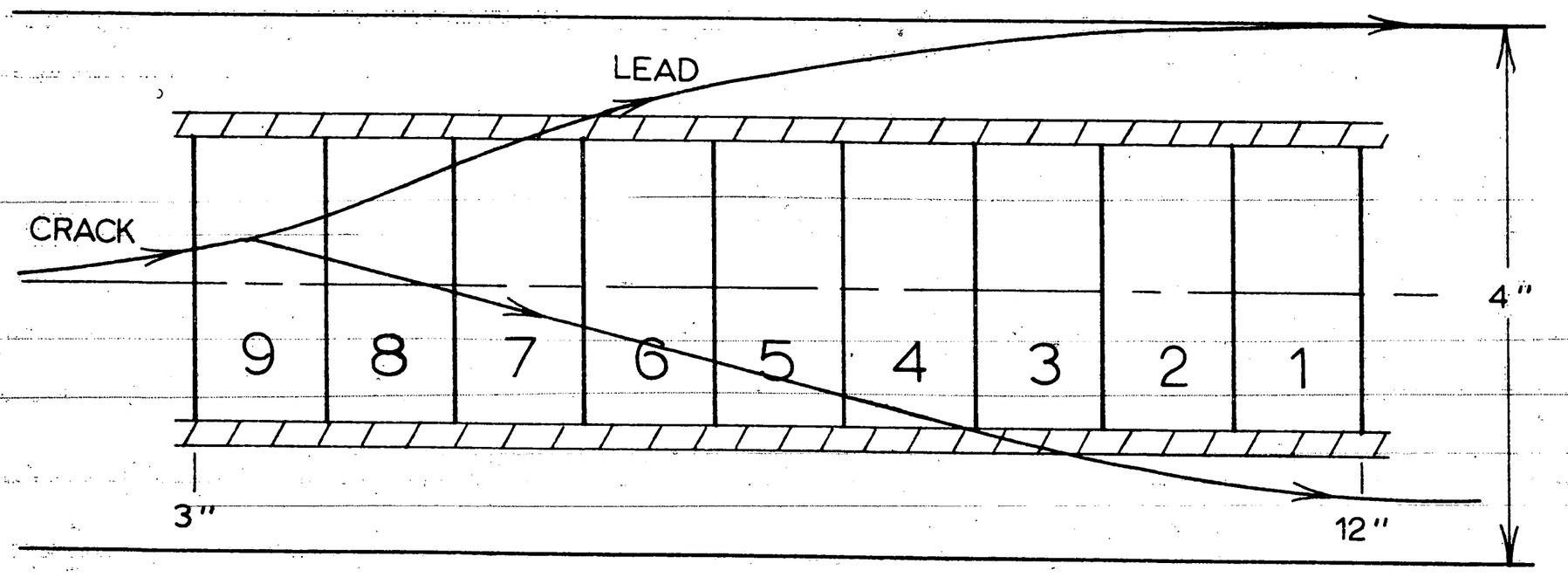

IX. FIGURES

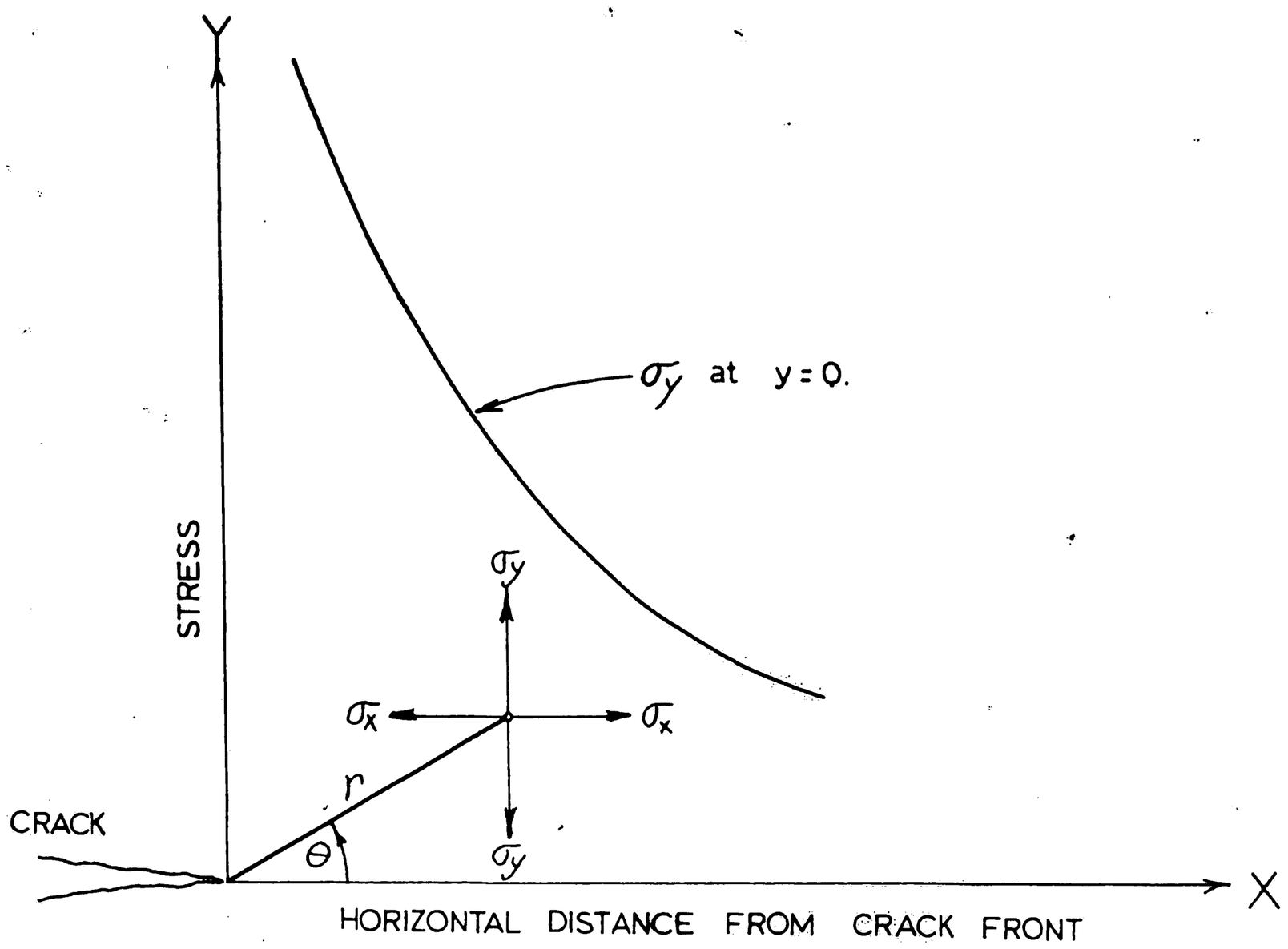

Figure 1a. Stress Conditions at the Crack Tip.

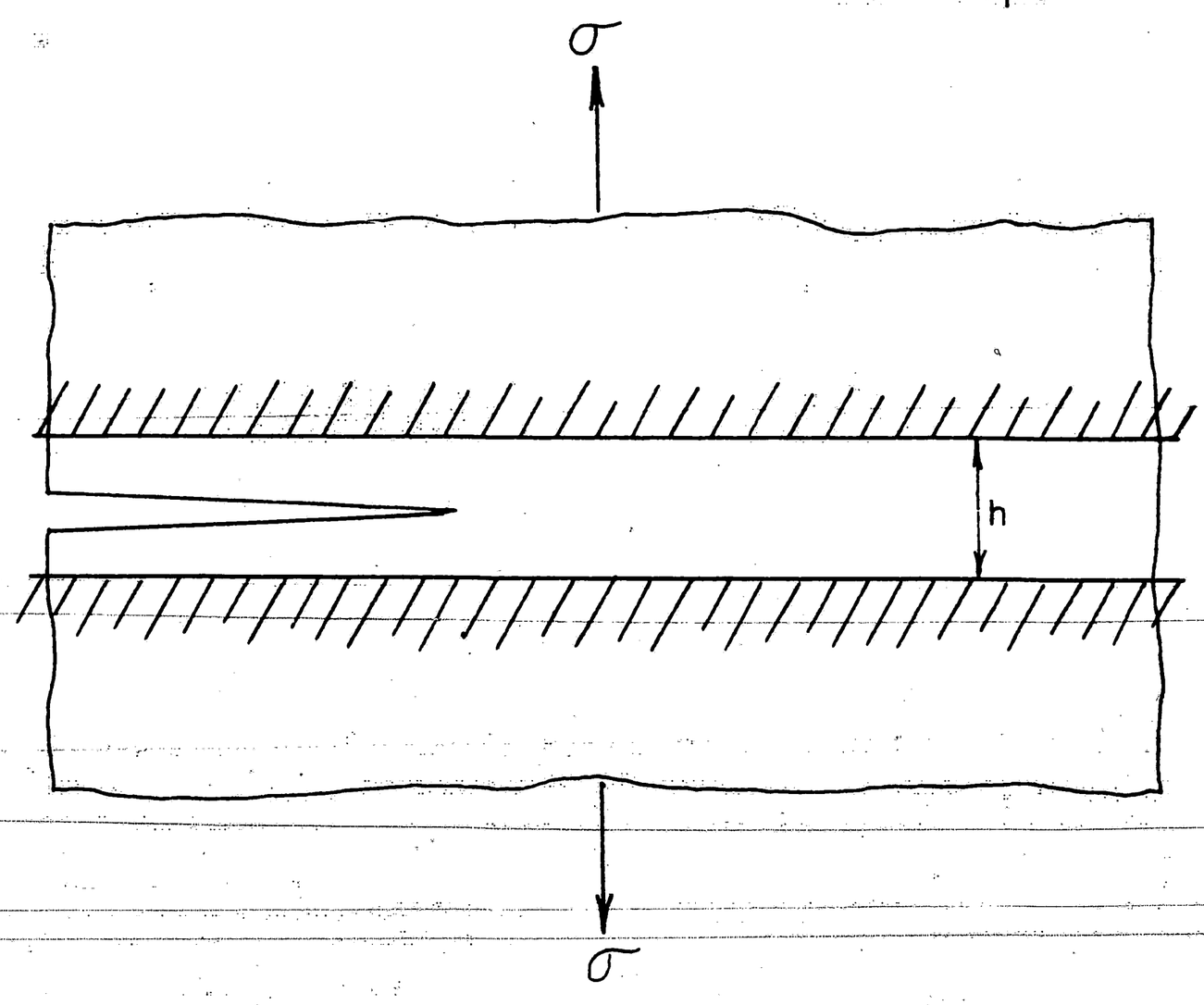

Figure 1b. The "Fixed Boundary Problem."

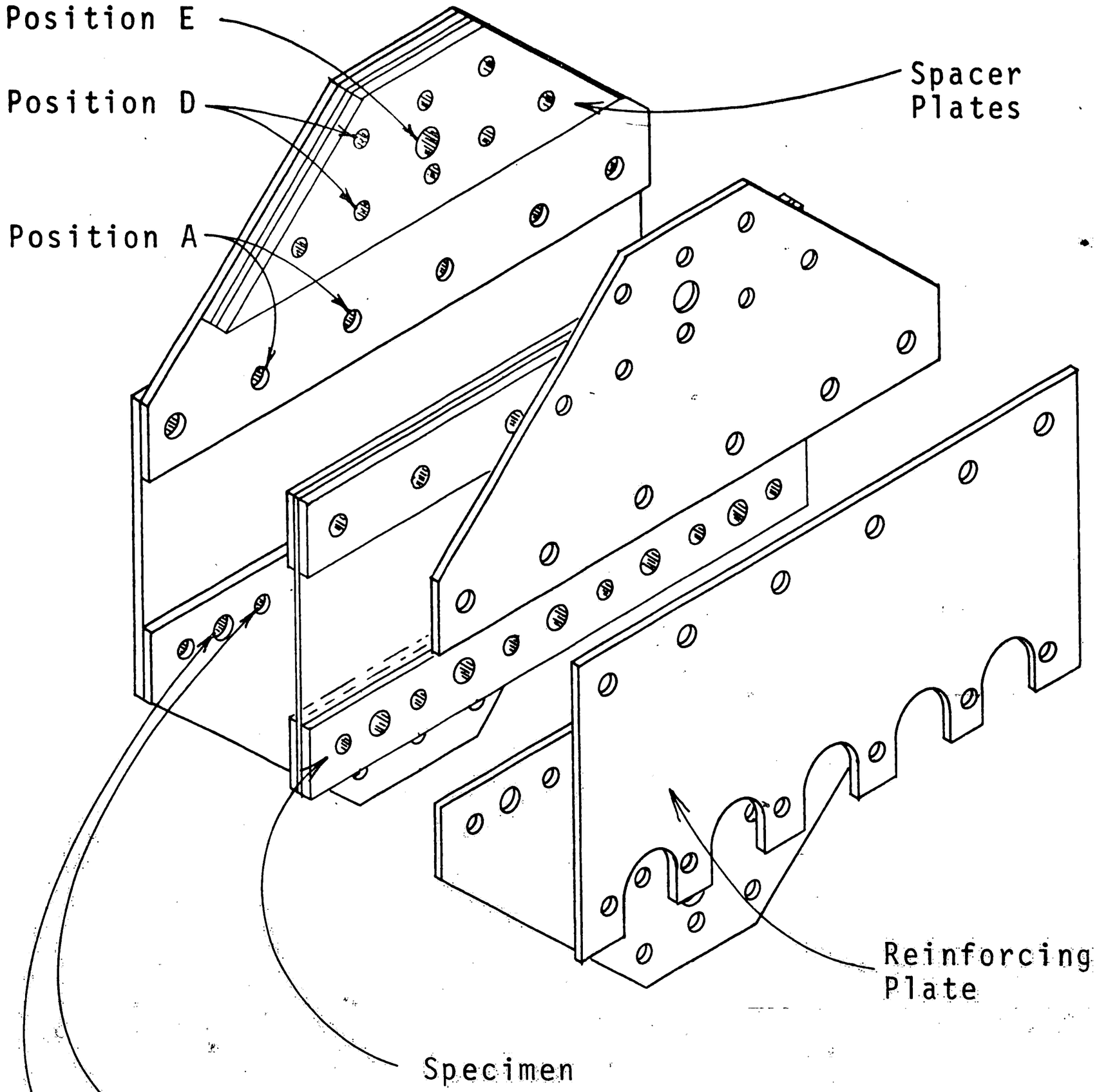

Figure 2. Exploded View of Test Frame and Specimen.

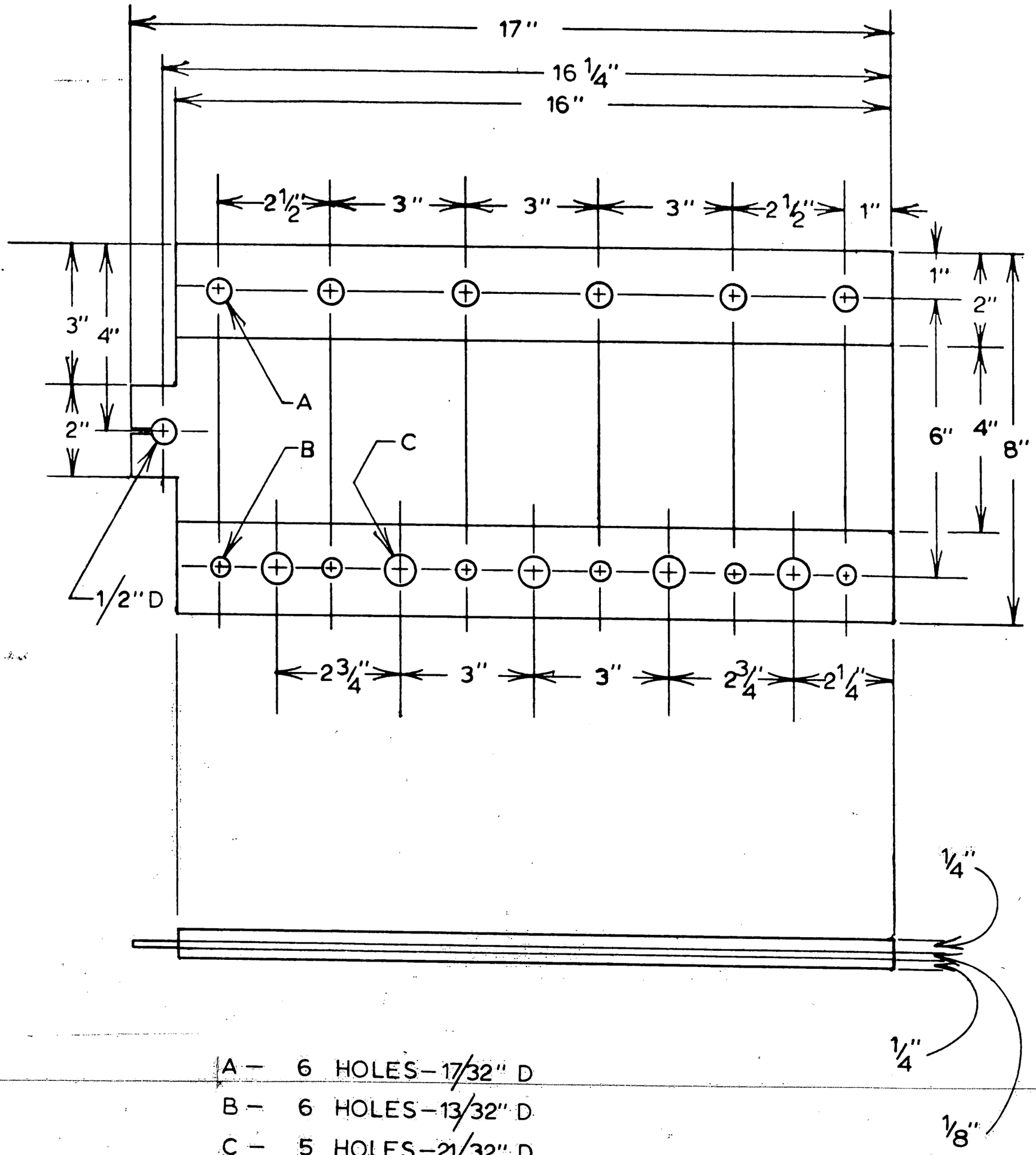

A — 6 HOLES — 17/32" D
B — 6 HOLES — 13/32" D
C — 5 HOLES — 21/32" D

Figure 3. Detailed View of Specimen.

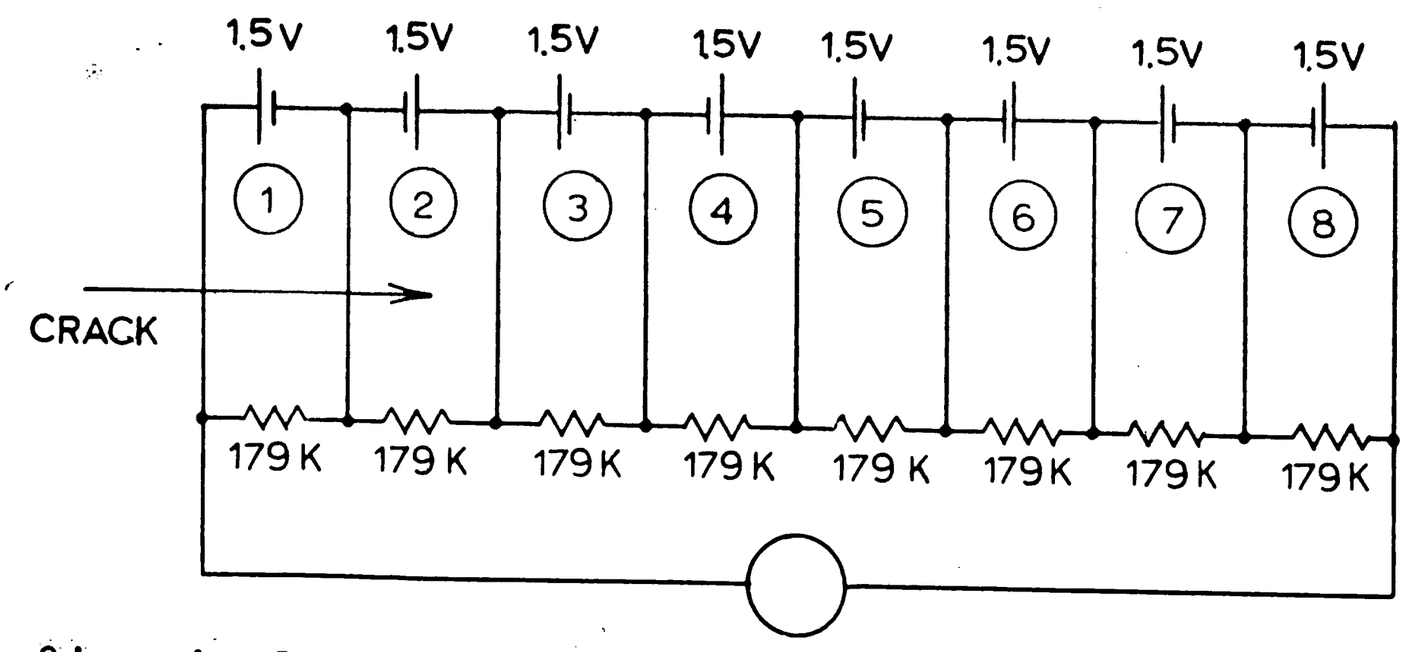

a. Circuit 1.

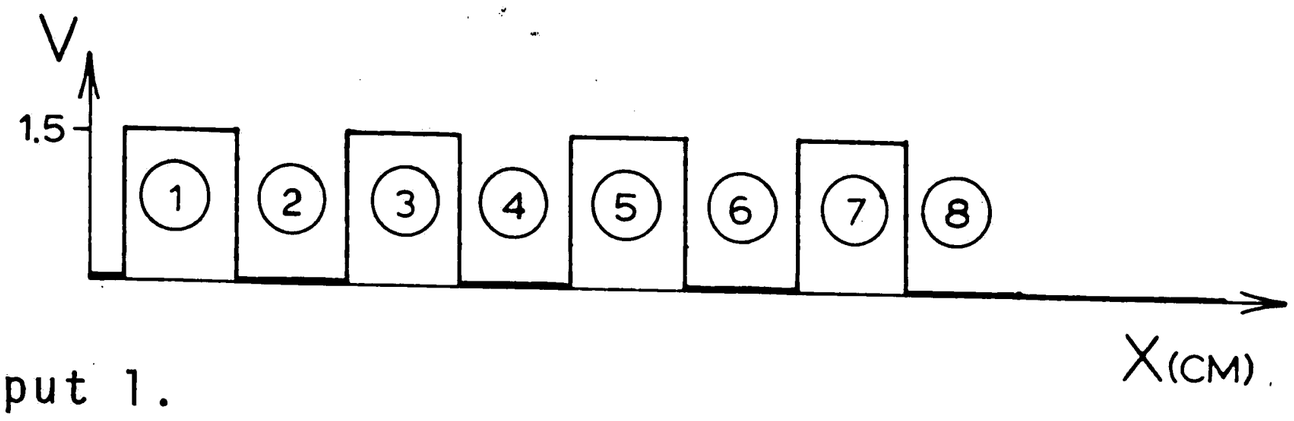

b. Output 1.

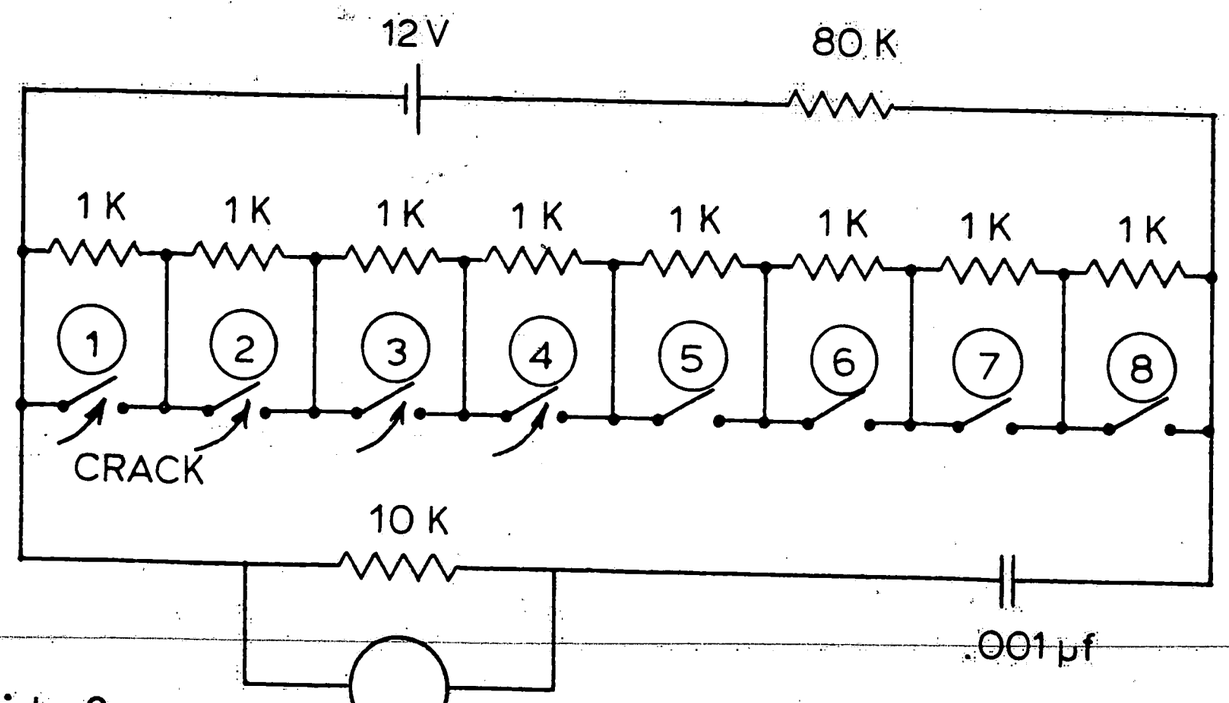

c. Circuit 2.

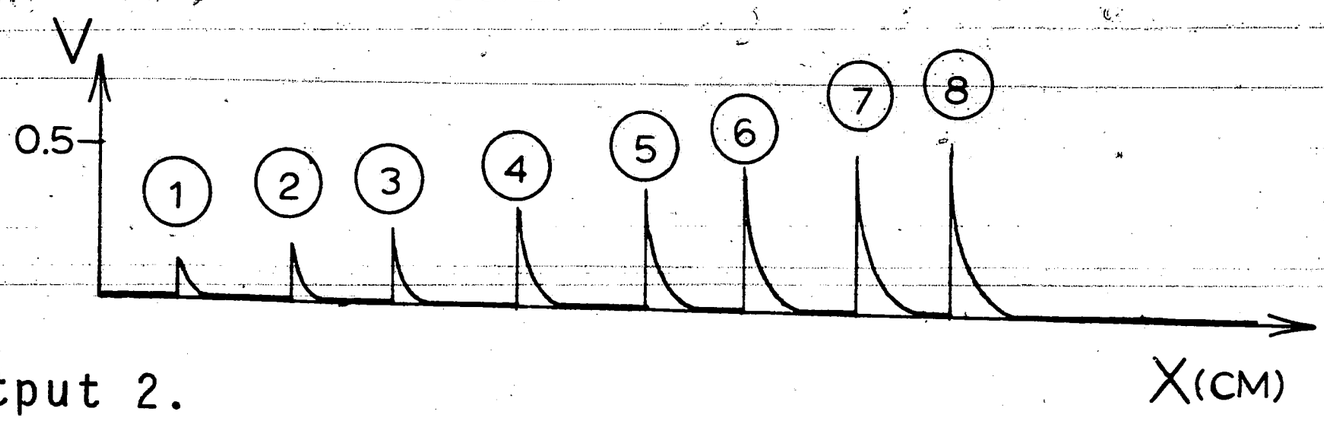

d. Output 2.

Figure 4. Velocity Meter Circuits and Corresponding Outputs.

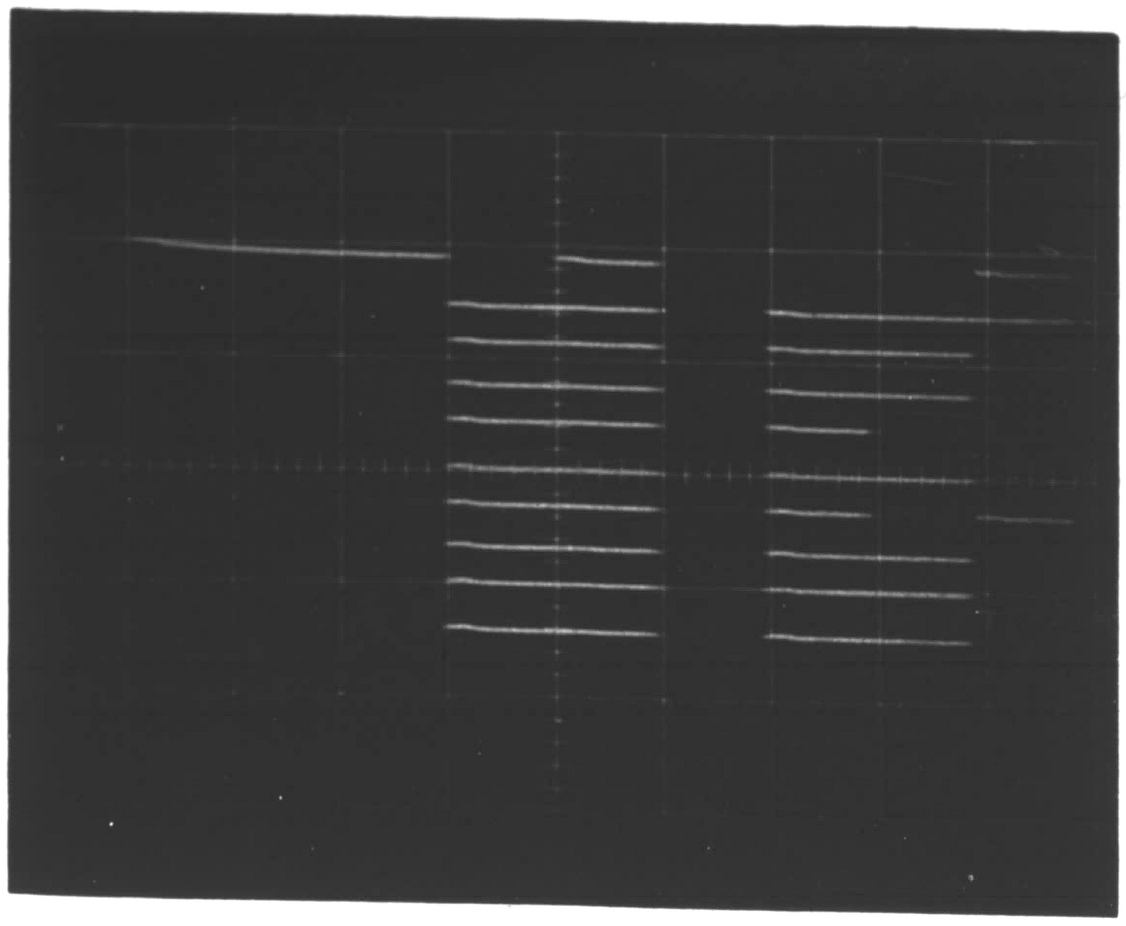

Figure 5. Sample Oscilloscope Record of Electronic Timer Output. (Test: 2500 psi.-- Standard Configuration -- See Table 7.)

INTERPRETATION

Binary Number	Correction	Decimal Number
0 1 1 1 0 1 0 0 0 1	-----	-----
0 0 0 0 1 1 0 1 1 1	+ 1	56
0 0 0 0 1 1 0 1 1 0	+ 1	55
0 0 0 0 1 1 0 1 1 0	+ 1	55
0 0 0 0 1 1 0 1 0 0	+ 1	53
0 0 0 0 1 1 0 1 1 0	+ 1	55
0 0 0 0 1 1 0 1 0 1	+ 1	54
0 0 0 0 1 1 0 1 1 0	+ 1	55
0 0 0 0 1 1 0 1 1 0	+ 1	55
0 0 0 0 1 1 0 1 1 0	+ 1	55

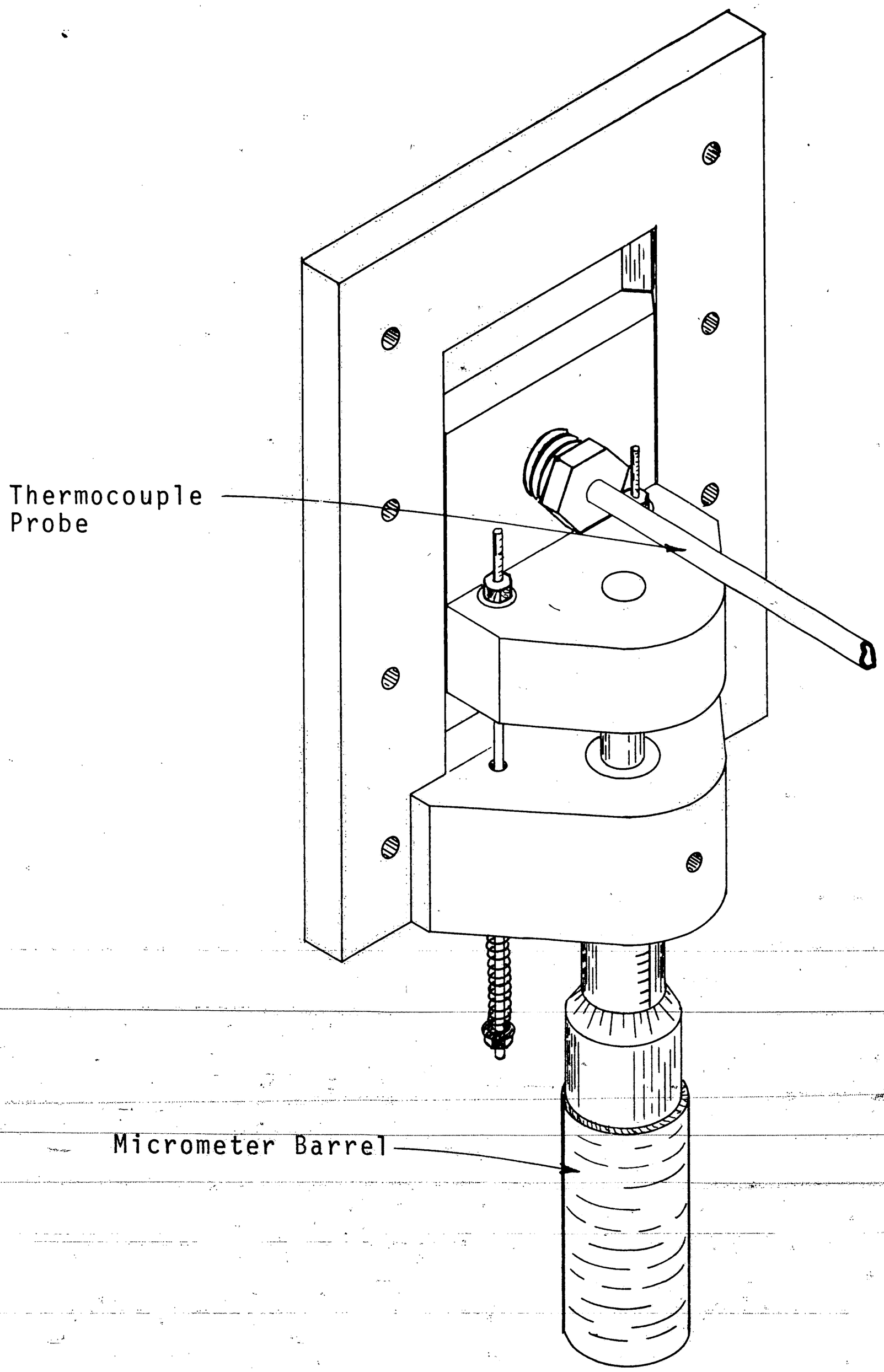

Figure 6. Probe Positioning Device.

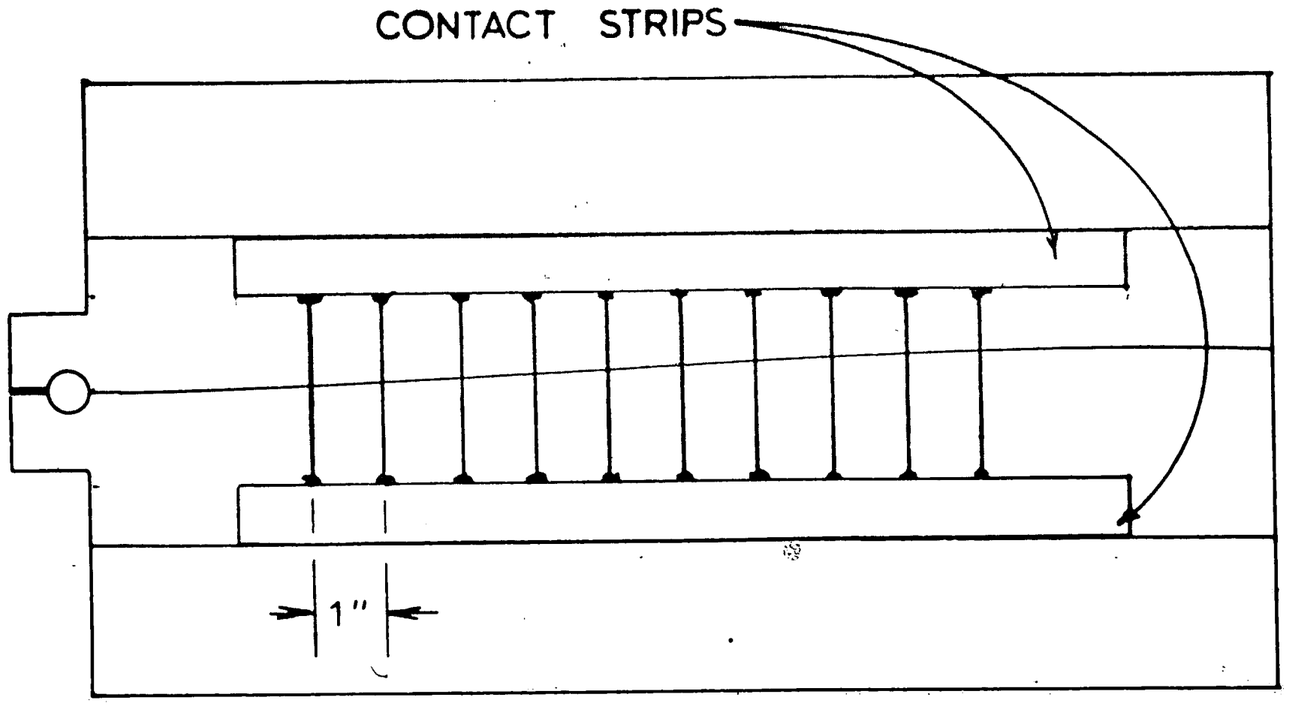

a. Standard Current Path Configuration.

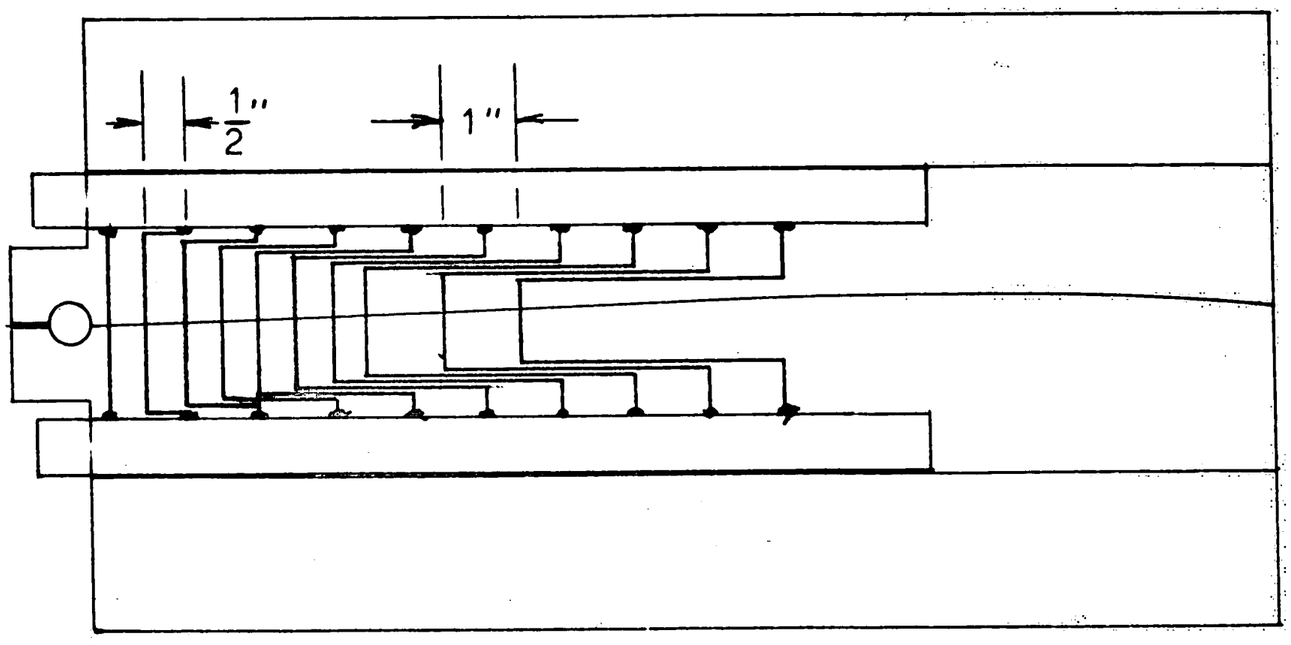

b. Current Path Configuration for Acceleration Test.

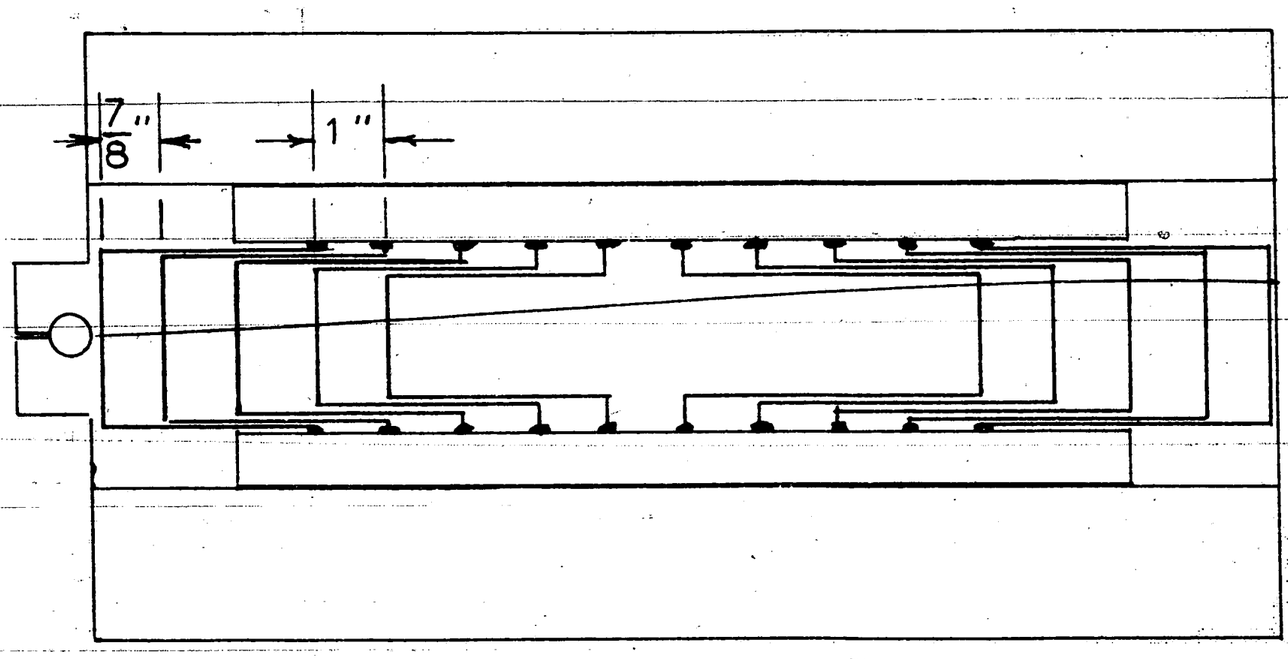

c. Current Path Configuration for V vs. Crack Length Test.

Figure 7. Layout of Current Paths

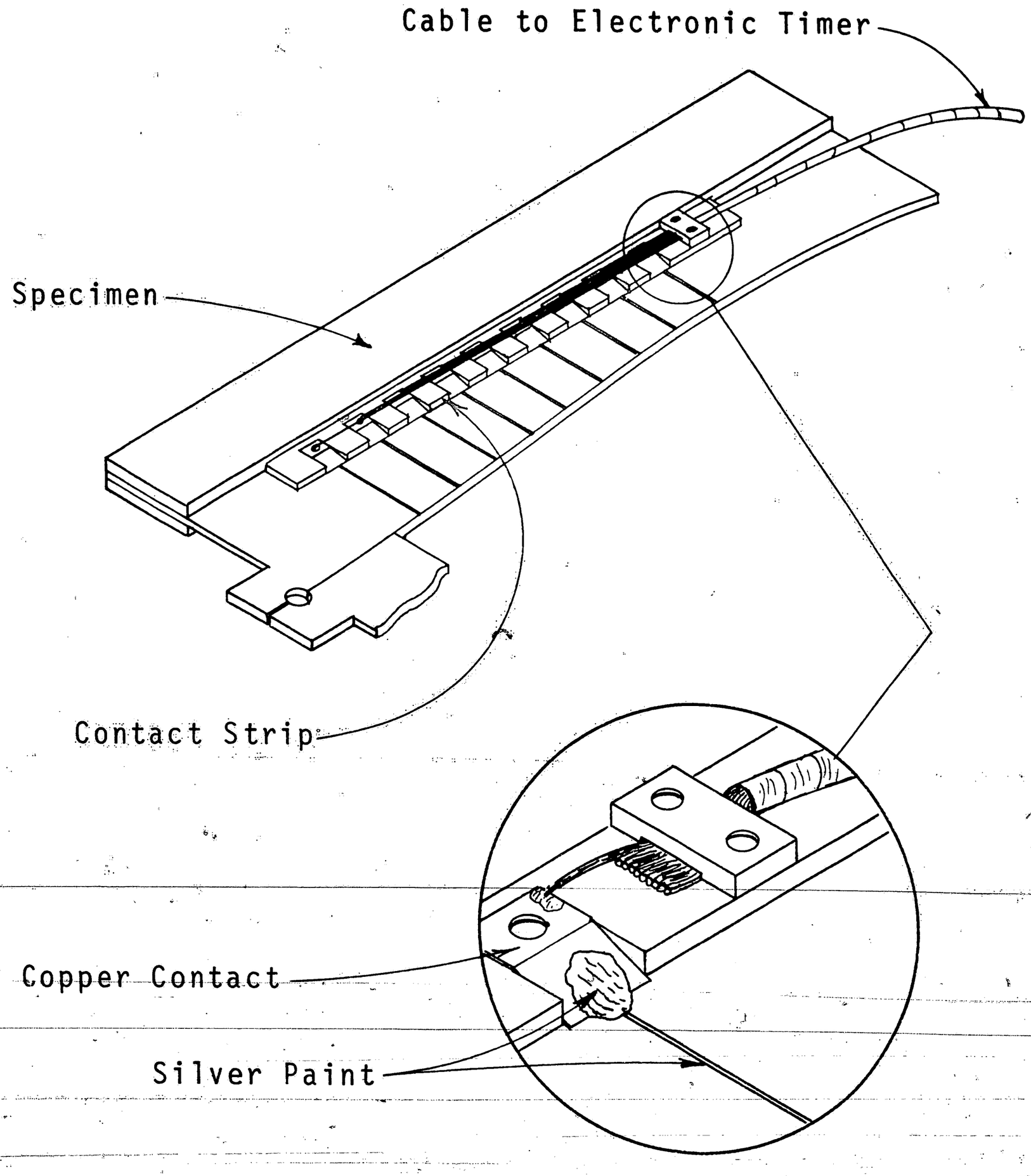

Figure 8. Contact Strips

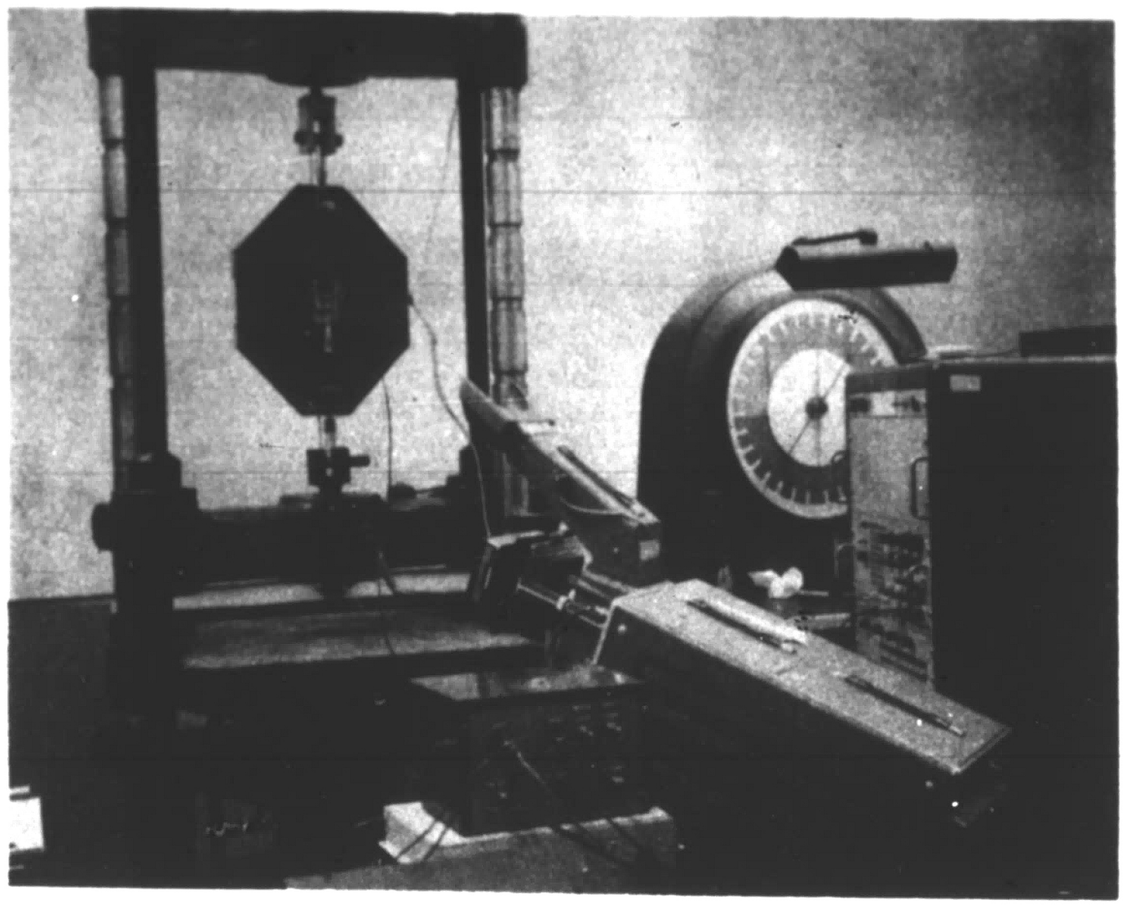

Figure 9. Overall View of Experimental Equipment: Including; Test Machine, Timer Instrumentation, and the Basic Temperature Measuring Apparatus.

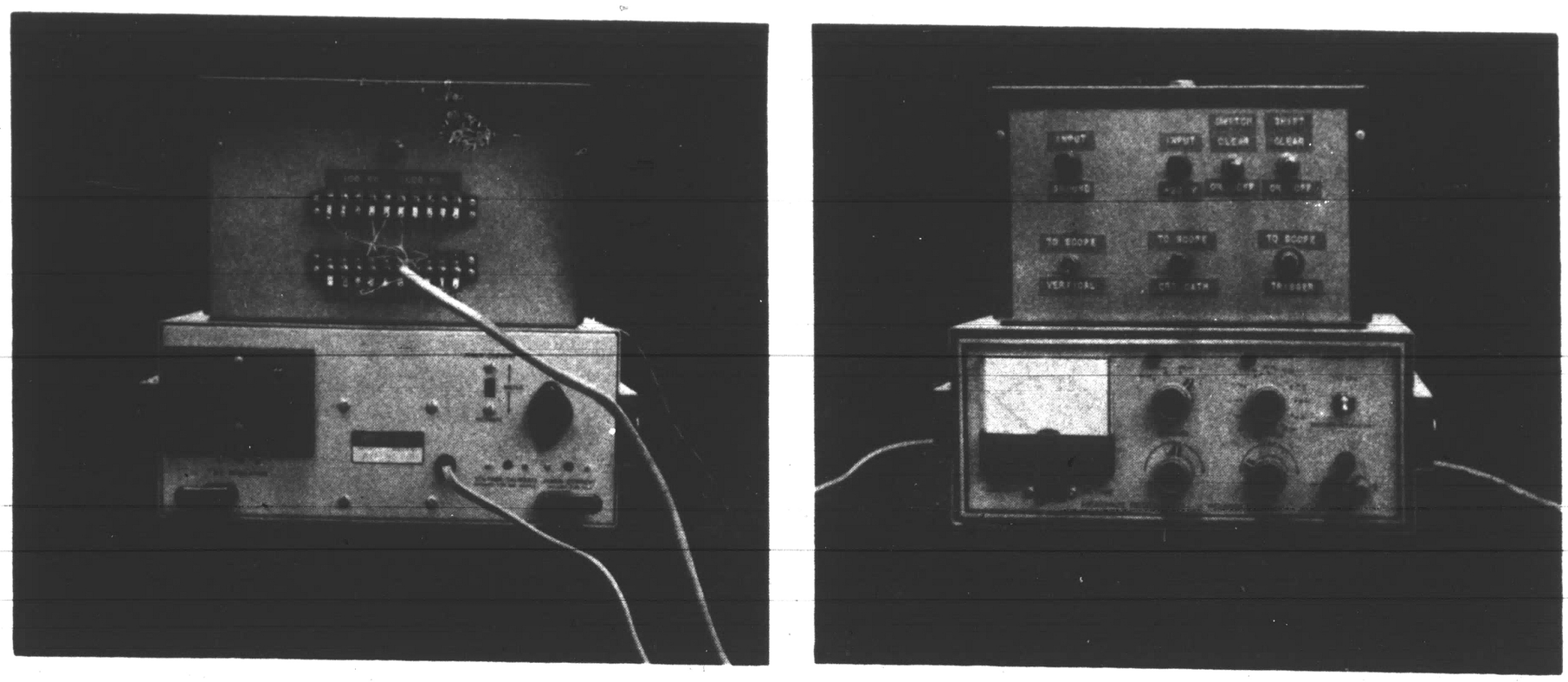

Back Front

Figure 10. Electronic Timer and Power Supply

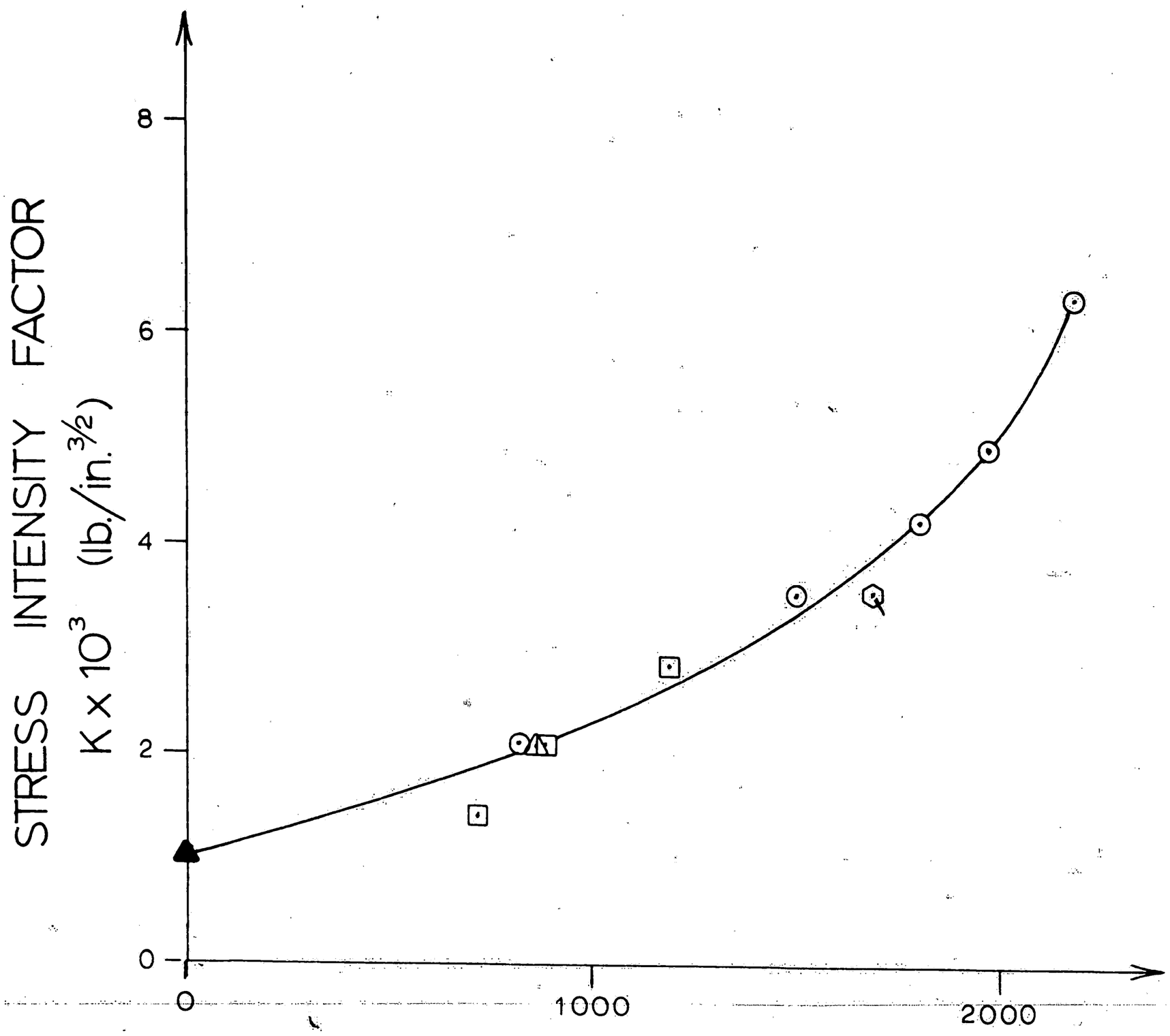

Legend:

▲ - Simple Tension Test.

⊡ - Crack Ran Out of Test Section.

△ - Wrong Timer Range Selected.

⊛ - Ununiform Plate Thickness.

⊙ - Acceptable Test.

Figure 11. Stress Intensity Factor versus Constant Section Velocity.

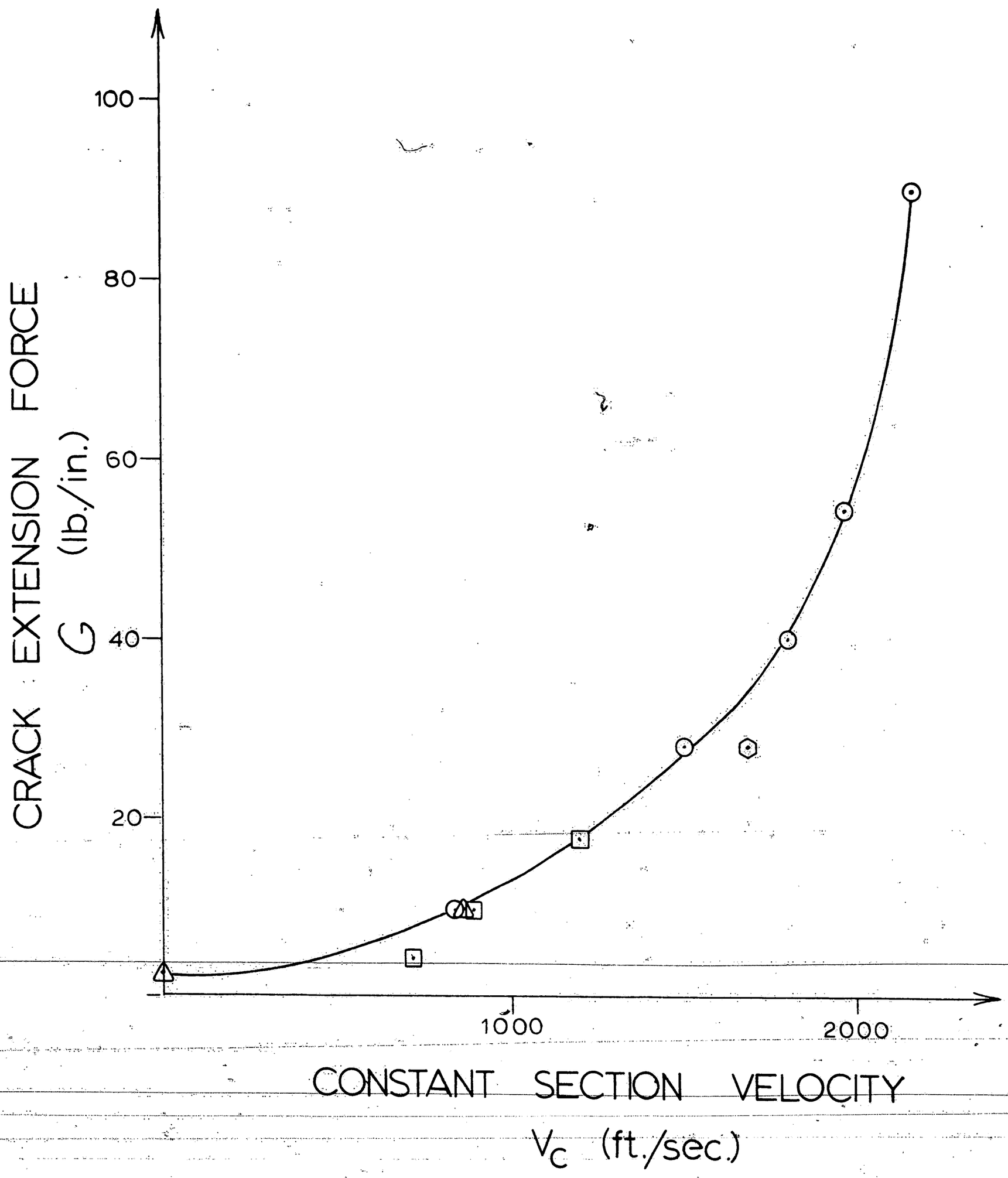

Figure 12. Crack Extension Force versus Constant Section Velocity.

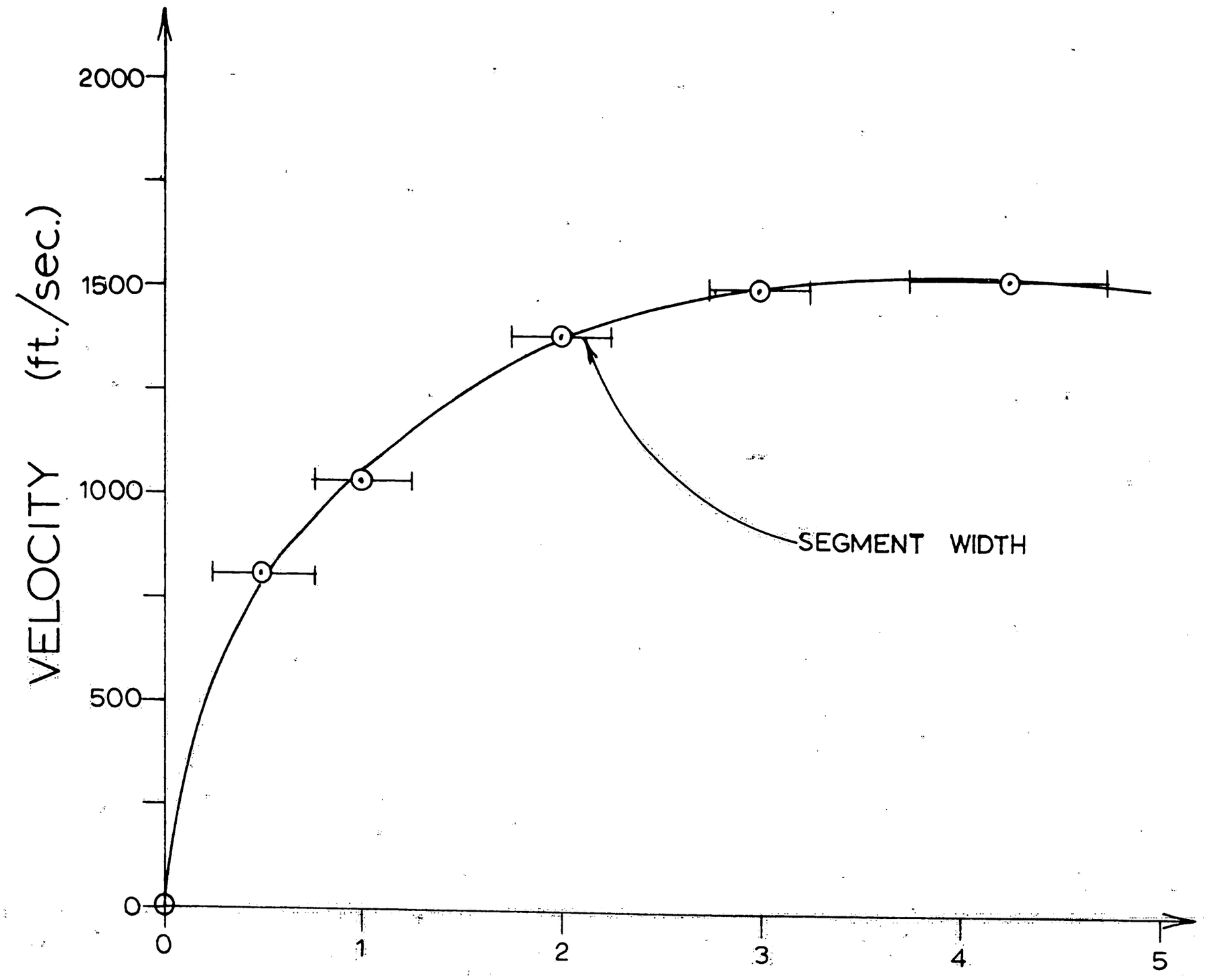

Figure 13. Crack Velocity versus Crack Length for the Acceleration Region -- at 2500 psi.

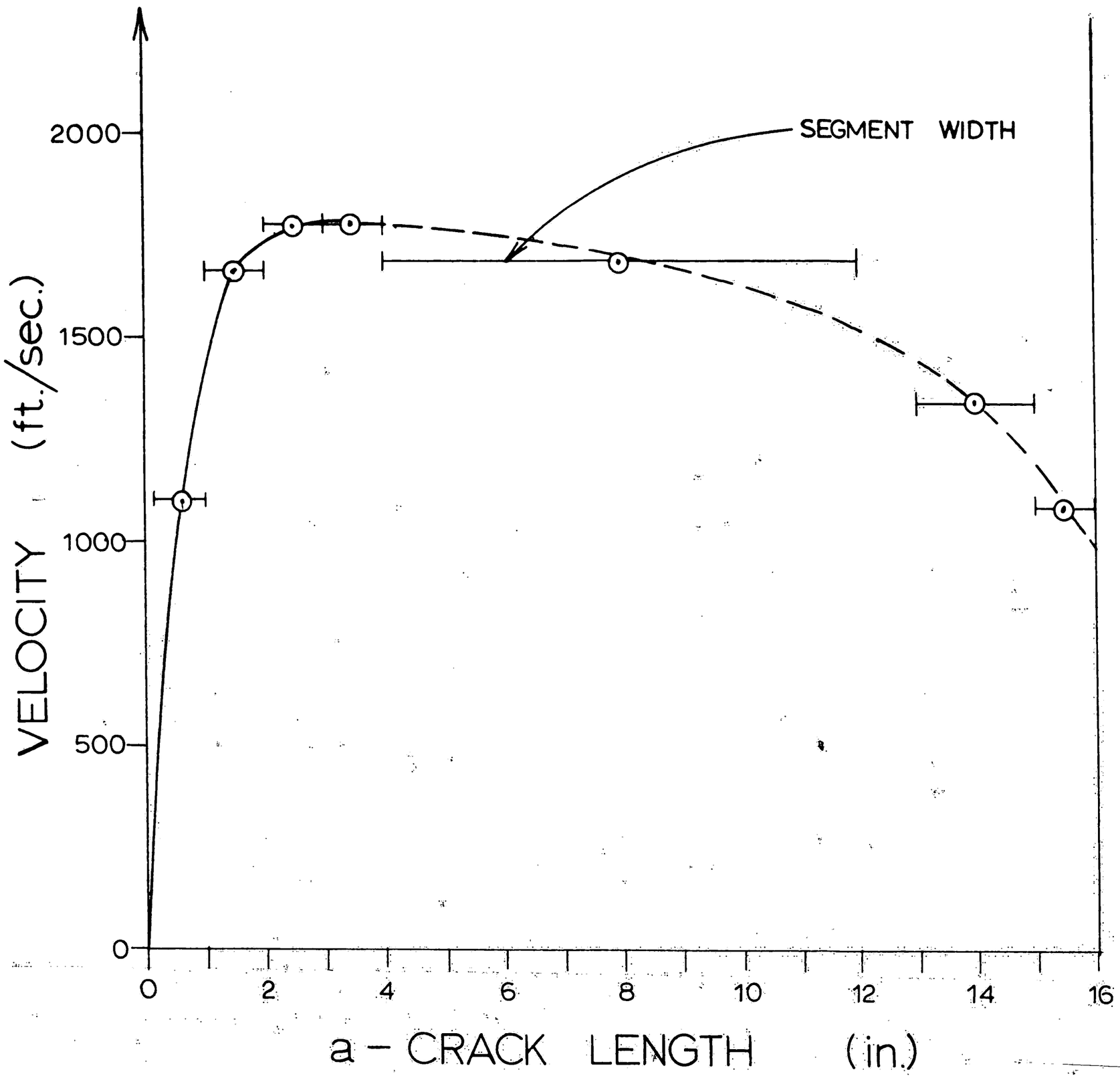

Figure 14. Crack Velocity versus Crack Length -- at 2500 psi.

X. APPENDICES

APPENDIX A.

Notation

Symbol	Description	Value (if fixed)
A	Cross sectional area.	2 $in.^2$ (nom.)
a	Instantaneous half crack length.	
a_o	Initial half crack length.	
a*	Thermal diffusivity = $\lambda/\rho c$.	$1.88 \times 10^{-4} \frac{in.^2}{sec.}$
c	Specific heat.	0.35 BTU/lb_m-°F.
C_1	Constant Energy value	
d	Perpendicular distance from the crack face.	
E	Young's Modulus.	4.5×10^5 psi.
$\mathcal{G}$	Crack Extension Force.	
$\mathcal{G}c$	Critical value of the Crack Extension Force.	2.36 lb./in.
K	Stress Intensity Factor.	
K_c	Fracture Toughness.	1030 $lb./in.^{3/2}$
k**	Numerical constant depending on the stress and displacement.	
P	Load.	
Q_F	Heat generated per unit crack length.	
t	Time.	
U	Temperature.	
U_{max}	Maximum temperature value.	
V_c	Constant section velocity.	
V_T	Terminal Velocity = $(2\pi E/k^{**}\rho)^{1/2}$	
z	Plate thickness.	0.125 in. (nom.)to (0.007 in.) under.
σ	Gross Stress.	
ρ	Density.	0.0426 $lb_m/in.^3$
λ	Thermal Conductivity	0.121 BTU/ft-hr-°F.
ν	Poisson's Ratio.	0.35

APPENDIX B.

Test Equipment

1. One Tektronix 535A oscilloscope with a Type G -- Plug-in and a Tektronix -- Series 125 oscilloscope camera with a Polaroid, pack film, backing.
2. One Baldwin 60,000 pound testing machine.
3. One Heathkit Low Voltage Power Supply, IP -- 27.
4. 36 Fairchild, μL923, J--K flip-flops, U8A992328X.
5. 46 Fairchild, μL914, Dual NOR Gates, U8A991428X.
6. One Fairchild TO-5 Voltage Regulator, U5R7723393.
7. One 1000kc. crystal and one 100kc. crystal.

APPENDIX C

A LOW-COST SUCCESSIVE-EVENT TIMER

by

W. A. BARRETT
Lehigh University
Bethlehem, Pennsylvania

INTRODUCTION

The measurement of successive contiguous time intervals in the microsecond to millisecond range occurs frequently in velocity and rate studies. An example in strength of materials studies is crack propagation across a flat specimen. The crack breaks filamentary current paths deposited on the surface of the specimen; the successive time intervals of path breakage are to be measured and recorded in some fashion.

The system described in this paper measures a time interval by counting clock pulses of a known frequency with a binary counter. At the end of a time interval (an event), the count is transferred to a recording system and the counter is reset to 0. The recording system consists of a shift register shifted continually by clock pulses, the last stage of which modulates the intensity of a cathode ray oscilloscope (CRO) trace. The shift register is loaded from the counter and the CRO trace is triggered by the event. The trace is also displaced downward by each event enough to separate the various time intervals. A display is complete in about 30 clock times.

Generally, the system fails if an interval is shorter than this; however, the existence of a failure is also clear from the scope display, so that no error can result from such a failure.

The system can accept almost any number of time intervals with very little additional circuitry needed for more intervals. The limit is set by the scope display, which becomes hard to read if too many are displayed. A reasonable upper limit is about 32 for a five-inch scope CRO. The system is almost completely made of inexpensive logic integrated circuits of two types, no critical adjustments are needed, and no logic hazards exist. The total component cost is about $300.00, using Fairchild industrial epoxy micrologic flip-flops and gates. The oscilloscope required should have a DC vertical sensitivity of at least 2v/division, a vertical display rise-time of 0.1μ sec. or less (if a 1 MHz clock is used), and a triggered, blanked linear sweep of 1μ sec/division. Fast recovery of the sweep circuit is essential to capture minimum time intervals.

SYSTEM DESCRIPTION

Figure 1A contains a schematic of the complete system, based on Fairchild NOR logic and J-K flip-flops. With these integrated circuits, a logical 1 is 1.3 volts or more, and a 0 is 0.3 volts or less. A dual NOR gate generates the Boolean function (A+B)', where A and B are the inputs. This means

the gate produces an output 1 only if both A and B are 0's. A single input NOR gate inverts the input logic. An open input behaves like a 0 input.

The J-K flip-flops used here are described by the truth table in Table 1A. The output X (pin 7) and its inverse $\overline{X}$ (pin 5) are unaffected by the inputs S, C and CP except during a logic transition of CP (pin 2) from a 1 to a 0. Thus, from the truth table, if S and C are both zeros, a CP transition 1→0 causes the flip-flop to change state. It is forced to a 0 if S = 0 and C = 1, and to a 1 if S = 1 and C = 0. Finally, the state is unaffected is S = C = 1.

The status of X persists for about 40 nsec after a CP transition, owing to internal delays in the flip-flop. This permits use of the previous state while CP is changing.

The flip-flop is unconditionally cleared by a 1 at P (pin 6). P must be 0 for the action of Table 1 to occur.

Several J-K flip-flops may be interconnected to form a binary counter. The event counter, EC1 - EC4 of Figure 1 is an example. Each stage has S = C = 0, hence each CP(1→0)* causes that stage to change state. Now CP for any one stage is X of the preceding stage. Hence, EC2 changes for every pair of changes of EC1, EC3 changes for every pair of changes of EC2, etc. If the counter is initially set to 0000, then

*Meaning terminal CP transfer from 1 to 0.

each CP(1→0) at pin 2 of EC1 causes the following sequence of states:

1000

0100

1100

0010

1010

etc.

1111

0000

This sequence is the sequence of the binary numbers 1, 2, 3, ---15, written backwards.

The interval counter IC1 - IC10 is made the same way. IC counts the 1→0 transitions of CLK, which is a square wave generated by a crystal-controlled oscillator G18 - G19.

The stages SR1 - SR9 and SRF10 comprise a shift register which may be loaded upon command (TR = 1) from the interval counter. Each stage consists of one J-K flip-flop and four dual-input gates. A shift register of 10 stages can hold a 10-bit binary number. Upon each shift command of CLK (1→0), the number is displaced one stage to the right; i.e., SR4 has the state that SR3 held formerly, etc.

If the shift register held the binary number

1011011101

initially, then a series of shift commands produces the states:

0101101110

0010110111

0001011011

0000101101

0000010110

0000001011

0000000101

0000000010

0000000001

0000000000

assuming the left end is filled with zeros. Note that the last flip-flop, SRF10, takes on a time-sequence of states that is exactly the initial binary number. Its output is therefore used (through Q7) to modulate the scope intensity to indicate a 1 or a 0.

States SR1 - SR9 act as a shift register when TR = 0. To see this, note that input S of SRF2 has the same value as X of SRF1, when TR = 0, and C is the inverse of S. Hence, if SRF1 holds a 0, S = 0 and C = 1 in SRF2. Then CLK (1→0) forces SRF2 to the state 0. Similarly, SRF2 is forced to a 1 if SRF1

held a 1. SRF1 is forced to 0 by CLK (1→0) when TR = 0.

When TR = 1 and CLK (1→0), each SR stage is forced to the state of the corresponding IC stage by the logic. This causes the IC contents to be transferred to SR.

In order that this works properly, the TR level must not change slightly in advance of CLK (1→0). The best time for a TR change is just after CLK (1→0). Now a TR pulse signifies a timing event, or the end of one interval and the beginning of the next. Since this can occur at any time relative to the CLK (1→0) transaction, it is necessary to synchronize TR so that it occurs within the nearest clock cycle and is timed properly within that cycle.

The retiming of TR is achieved by the input flip-flops INF1 - INF10 and TRF. Note that for TRF, C is always $\overline{S}$. Also, if TR = 1, all the flip-flops INF1 - INF10 are cleared through gates G4, G2 and G3. When INF1 - INF10 are cleared, input S of TRF is 0 and C is 1, hence, TRF is cleared by the next CLR (1→0), removing the clear signal from INF1 - INF10. With the clear removed, a time event causes CP of one of the flip-flops INF1 - 10 to change from 1 to 0 (one of the switches is opened which trips the corresponding input flip-flop). Since the inputs S = C = 0, the INF flip-flop is set, and pulls up S of TRF. TRF then is set at the next CLK (1→0) time. It should now be clear that TR is normally 0, it changes to 1 for exactly one clock time, is synchronized with the clock tran-

sitions and occurs in the nearest clock interval following the event.

Nor TR (0→1) causes the event counter EC to advance one count. With TR = 1, the interstage logic in SR is set up for a transfer on the next CLK (1→0). The transfer has not yet occurred, because TR (0→1) lags CLK (1→0) by about 40 nsec.

The output of the event counter EC is connected to transistor switches Q3 - Q6. A switch is "open" if its EC stage holds a 0, and "closed" if that stage holds a 1. Because of the sizes or resistors R3-6, the emitter current in Q2 is proportional to the magnitude of the binary number in EC. This current is seen as a proportional voltage at the collector of Q2 and is used to deflect the trace vertically to separate the successive timing intervals.

Just before TR (1→0) occurs, the contents of IC is transferred to SR by a CLK (1→0). Then TR (1→0) sets the clear flip-flop CLF, which causes IC1 - IC10 to be cleared. The clear persists until CLK changes to 1, which also resets CLF. Because of the clear, one clock count is lost for each TR pulse, which should be added to the number finally displayed.

TR (0→1) is also used to trigger the scope sweep through the switch Q1. Since the transfer is not completed till TR (1→0), the first clock time of the scope display should be a zero, and signifies nothing.

INTERPRETATION OF THE SCOPE DISPLAY

An illustrative scope display is shown in Figure 2A. It consists of a series of horizontal traces, each displaced by about 1 volt downward from the preceding trace, and intensity modulated. Each trace represents the time interval, in clock period units, between two events, coded in binary form, reading from left to right. The first displayed bit (bit 0, Figure 1) is ignored, and the remaining group (bits 1 - 10) represents the desired number. Unity should be added to each number for an unbiased time measurement accurate to $\pm$ clock periods maximum error.

Trace 1 in Figure 2 is meaningless, as it represents a "stop" with no "start" other than turning on the system power.

Trace 5 shifted down 7 time units after it started. This means a new event occurred while the previous one was being displayed. Its time can be judged from the sweep speed; however the measured time for the one being displayed is largely lost due to a loss of information in SR.

The missing trace (trace 8) means that an event occurred while the scope sweep circuit was recovering. That time is lost, though one may place bounds on it if something is known about the sweep recovery time.

With these guidelines, the following may be inferred from Figure 2:

Trace	Meaning
1	meaningless
2	interval 1 time = 1101100 + 1 = 109 units
3	interval 2 time = 1011110 + 1 = 95 units
4	interval 3 time = 1110011 + 1 + 116 units
5	interval 4 time approximately 1100000 = 96 units
6	interval 5 time 7 units (7 divisions)
7	interval 6 time = 111110 + 1 = 63 units
8	interval 7 time unknown, probably 10-20 units
9	interval 8 time = 110101 + 1 = 54 units
10	interval 9 time = 1100100 + 1 = 101 units
11	interval 10 time = 1011001 + 1 = 90 units

SYSTEM VARIATIONS

It is clear that several arbitrary choices were made in the system of Figure 1. A 10-stage interval counter can register up to 1024 clock times. Each additional stage would double the maximum count. Similarly, the number of events possible is arbitrary and may be increased by adding more EC stages. However, more stages requires more care to adjust the binary converter resistors to obtain an evenly spaced trace. Additional EC stages should be added to the left side of EC with

converter resistors 12K, 24K, etc.

Several variations are possible on the input. The double flip-flop shown was chosen to catch a "slowly varying" input voltage rise once and only once. The clock input (CP) of the Fairchild JK flip-flop must change from 1 to 0 in less than 40 nsec., or it is ignored. Hence, the input set-reset flip-flop. A fast input voltage source could go directly to the CP terminal of the JK flip-flop. Also a single input that changes periodically with a fast fall time would require only one flip-flop.

Lower clock frequencies are easily arranged by changing the crystal. Frequencies higher than 2 MHz should not be used with these logic packs, owing to the counter ripple propagation time (about 400 nsec., for a 10-stage counter). Other logic circuits, such as TTL, are available for counting up to 20 MHz.

SOME CAVEATS

Logic pack loading rules must be observed in any modification of the system of Figure 1a. In general, an expansion in size calls for a reassessment of gate loading. Most of the single-input gates in Figure 1 are to assure in-tolerance loading of each logic pack.

The NPN transistors used should be silicon, and have $\beta>20$, $BV_{cbo}>30v$ and $f_T>100$ MHz. The power sources of 3.6v and 20v

should be regulated. The 3.6v source drain is about 650 ma, and the 20v source drain 20 ma(max.). The 3.6 volt source should be decoupled with a 0.1 μf ceramic capacitor located close to a group of logic packs. One capacitor for each 5-10 packs should be adequate. Ground leads should also follow signal leads from pack to pack.

S	C	X_{n+1}
0	0	$\overline{X}_n$
0	1	0
1	0	1
1	1	X_n

Table 1A. Truth Table for J--K flop-flop, μL923. X_{n+1} is the state of X(pin 7) upon transfer of CP(pin 2) from 1 to 0, or it depends on S(pin 1) and C(pin 3). The former state persists for about 40 nsec. after the CP transition.

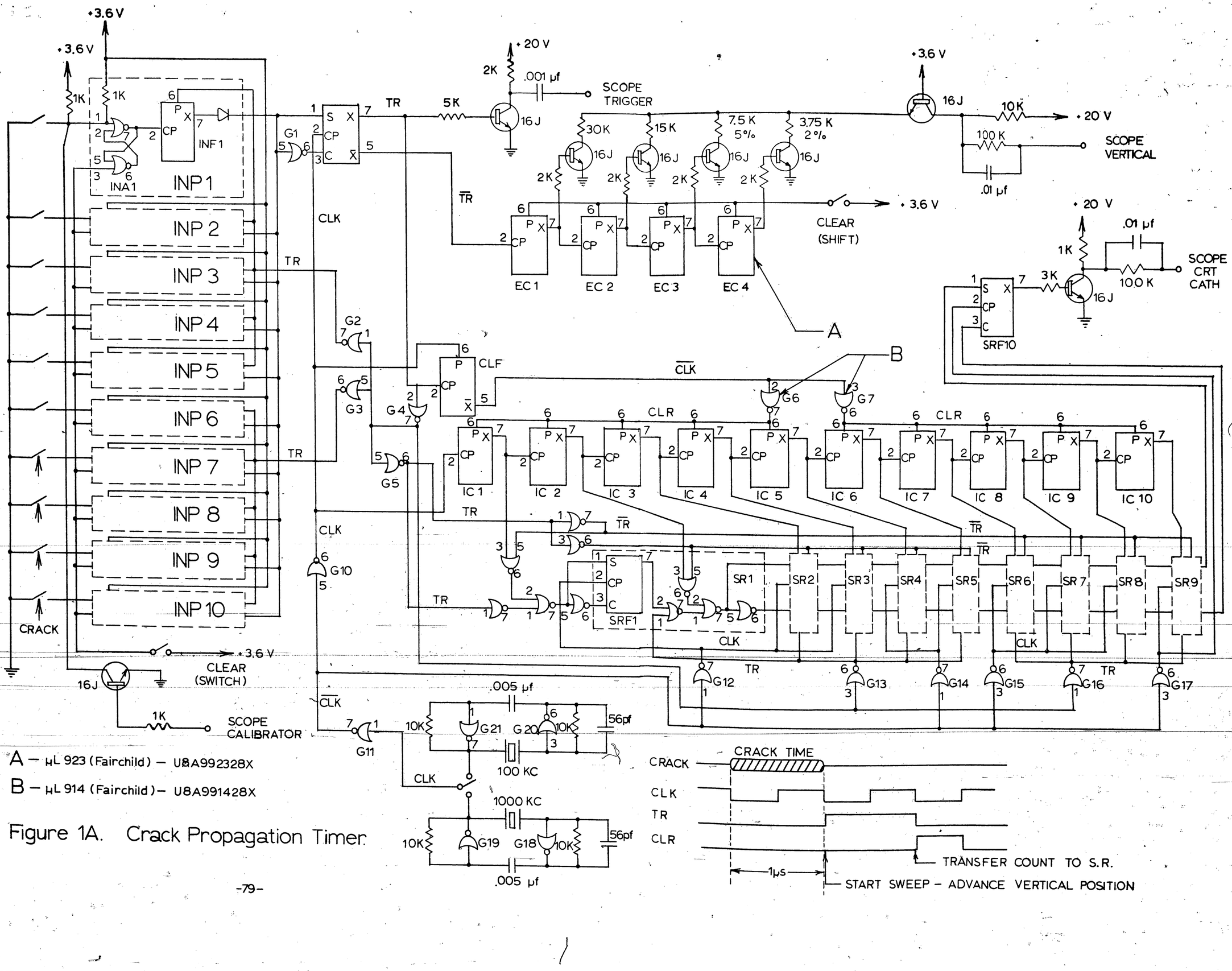

A – µL 923 (Fairchild) – U8A992328X

B – µL 914 (Fairchild) – U8A991428X

Figure 1A. Crack Propagation Timer

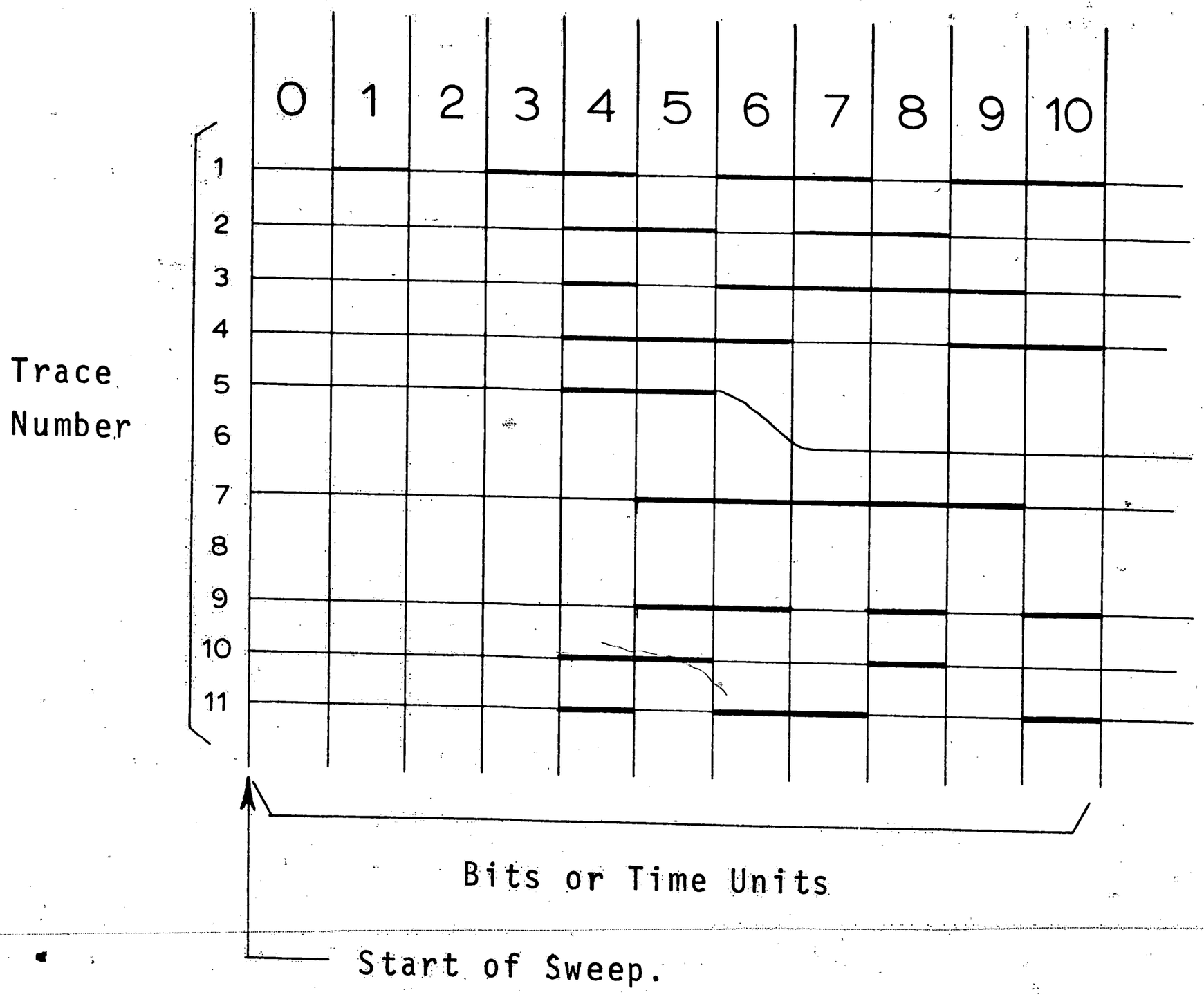

Figure 2A. Illustrative scope trace generated by the timing system of Figure 1A, and a sequence of ten events. See text for interpretation.

APPENDIX D

TEST PROCEDURE CHECKLIST

A list of the operations and inspections which had to be completed to insure successful tests is given below. An explanation is included where the operations are not obvious. The order of presentation is identical to that used in the actual procedure.

CONNECTIONS:	Check connections at timer and CRO.
1. Scope Vertical	
2. Scope Trigger	
3. Scope Crt. Cath.	
4. Ground	
5. + 20 Volts	From power supply.
6. Cable Tabs	Timer input terminals.
SPECIMEN:	Preparation.
7. Clean	Examine test section surface and clean if necessary.
8. Saw Cut	1/64" to 1/16" long.
9. Contact Strips	Place on specimen and paint up the ramps. (Paint on current paths beforehand).
10. Continuity	The resistance of each current path (including cable) must be less than 30 ohms.

TEST FRAME:

11.	Alinement	Place specimen in load frame and insert all bolts.
12.	Bolts Tight	45 ft.-lbs. torque on bolts in position A -- move frame to test machine and mount it -- 45 ft.-lbs. torque on bolts in position C.
13.	6 Bolts Loose	Loosen two outside bolts (position B) which were tightened before moving the frame to prevent specimen damage.
14.	Cables Straight	Loading Cables.
15.	Cable Clear	Check that timer connecting cable is suspended and secure.

EQUIPMENT:

16.	Baldwin On	Testing Machine.
17.	Scope On	Oscilloscope (CRO) On.
18.	Power On	A.C. current to Power Supply.
19.	VTVM On	
20.	Air On	For testing machine load indicator.
21.	Clock Range	Set electronic timer range to either 1000 kc. or 100 kc.
22.	Check Film	In oscilloscope camera.

SCOPE: Oscilloscope settings for a Tektronix 535A.

23.	Trigger Mode	A.C.
24.	Trigger Slope	Negative.
25.	Time/Cm.	10μ sec./cm. for 100 kc. crystal; 1μ sec./cm. for 1000 kc. crystal.
26.	Variable	Calibrated.
27.	Horiz. Display	A.

28.	x5 Mag.	Off.
29.	Volts/Cm.	2 volts/cm. (Plug-in amplitude control).
	POWER SUPPLY:	
30.	Course Voltage	20 - 25 volts.
31.	Fine Voltage	Adjust to + 20 volts.
32.	Course Current	1.5 amps.
33.	Fine Current	Adjust so that + 20 volts is just supplied.
34.	Stand-by	Turn off current to timer.
	CLOCK:	
35.	Con. Calib.	Connect calibrator circuit (CRO) to the electronic timer.
36.	Sh. Clear (Off)	Open "Shift Clear" switch.
37.	Sw. Clear (On)	Close "Switch Clear" switch.
38.	Tab 1 Off	Unfasten lead to terminal 1. (Disconnects timer from current path on specimen).
39.	Scope Cal. 2v.	Oscilloscope calibrator amplitude setting.
40.	Power On	Current supplied to timer -- produces test pattern on CRO screen.
41.	Adj. Horiz.	
42.	Adj. Vert.	
43.	Focus	Adjustment of test pattern on CRO screen.
44.	Intensity	
45.	Astigmatism	
46.	Illum. Off	CRO grid illumination off.

47.	Scope Cal. Off	Calibrator of "Off" position.
48.	Tab 1 On	
49.	Check Bias	Voltage across input terminals must be less than 0.1 volt.
50.	Clear	Close and then open both "Switch Clear" and "Shift Clear" switches.
51.	Power Off	Same as Stand-by. (No. 34).

CAMERA:

52.	f - 2.7 -- 3.0	Camera f-stop adjustment; 2.7 for the 1000 kc. range and 3.0 for the 100 kc. range.
53.	Shutter - T	Manual shutter control.
54.	Door Shut	Observation Port door closed.

TEST:

55.	Load Specimen	Preload to 100 lb., plumb, and then load to test load.
56.	Hold Load	At the test load.
57.	Tighten Bolts	Tighten bolts in position B to 35 ft.-lbs.
58.	Record Time	Hold time.
59.	Power On	
60.	Pull Slide	On camera.
61.	Check Bias	Same as above.
62.	Clear	Same as above.
63.	Open Shutter	Open camera shutter.
64.	Start Crack	Place wedge directly in saw cut and tap lightly with a hammer.
65.	Close Shutter	

66.	f - 8	Reset camera and CRO to place grid on photograph.
67.	Illum. 11 - 22	
68.	Shutter - 1 sec.	
69.	Trip Shutter	
70.	Remove Picture	
71.	Check Cont.	Check continuity to determine which current paths have been severed.
72.	Power Off	Shut down system.

XI. REFERENCES

1. Mott, N. F., "Fracture of Metals: Theoretical Considerations", ENGINEERING, 165, p. 16, (1948).

2. Roberts, D. K., and Wells, A. A., "The Velocity of Brittle Fracture", ENGINEERING, 178, p. 820, (1954).

3. Dulaney, E. N., and Brace, W. F., "Velocity Behavior of a Growing Crack", J. Appl. Phys., 31, p. 2233, (1960).

4. Maxwell, B., J. Soc. Plastics Engrs., 15, p. 480, (1959).

5. Manitz, Gerhart, "Uber den Bruchvorgang Bei Verschieden Hochpolymeren", Unpublished Ph.D. dissertation, Albert-Ludwigs- Universitut. zu. Freiburg i. Br., (1959).

6. Cotterell, B., "On the Nature of Moving Cracks", J. Appl. Mech., Trans. ASME, 31, p. 12, (1964).

7. Cotterell, B., "Velocity Effects in Fracture Propagation", Appl. Matls. Research, 4, p. 227, (1965).

8. Song, W. C., "The Velocity Variation of Crack Propagation in an Aluminum Sheet with Fixed Boundaries", Unpublished Masters Thesis, University of Washington, (1960).

9. Paris, P. C., "Initiation, Propagation, and the Arrest of Fractures in Aircraft Metals", A Report to Boeing Airplane Company, (1955).

10. Paris, P. C., and Whitmore, C. F., "Tear Resistance and the Effect of Nominal Stresses", An Unpublished Paper, University of Washington, (1959).

11. Shannon, J. L., "Fracture Mechanics, I", Machine Design, 23, p. 122, (1969).

12. Paris, P. C., and Sih, G. C. M., "Stress Analysis of Cracks", Reprint from Symposium on Fracture Toughness Testing and its Applications, No. 381, ASTM, (1965).

13. Clark, A. B. J., and Irwin, G. R., "Crack-Propagation Behaviors", J. Soc. Exper. Stress Analysis, 6, p. 321, (1966).

14. Carslaw, H. S., and Jaeger, J. C., Conduction of Heat in Solids, 2nd Ed., New York: Oxford University Press, (1959).

15. Schneider, P. J., Conduction Heat Transfer, Reading, Mass., Addision Wesley Publishing Company, Inc., (1961).

16. Erdogan, F., "Crack Propagation Theories", Rep. Dept. Mech. Lehigh University, (1967).

17. Lucas, R. A., "A Quasi-Static Thermoelastic Analysis of a Propagating Crack", Int. J. Solids Structures, 5, p. 175, (1969).

18. Irwin, G. R., Krafft, J. M., Paris, P. C., and Wells, A. A., "Basic Aspects of Crack Growth and Fracture", N.R.L. Report 6598, (1967).

19. Pierson, O. L., "Acrylics", Machine Design (Reference Issue on Plastics), 4th Ed., 29, (1968).

20. Boyd, G. M., "The Conditions for Unstable Rupturing of a Wide Plate", Trans. Inst. Naval Architects, 99, p. 349, (1957).

21. Erdogan, F., Tuncel, O., and Paris, P. C., "An Experimental Investigation of the Crack Tip Stress Intensity Factors in Plates Under Cylindrical Bending", ASME Paper No. 62-Met-5, (1962).

22. Watson, C., "Design of a Test Frame and Specimen for the Fixed Boundary Fracture Problem", Unpublished ME. 109 Report, Lehigh University, (1968).

23. Rice, J. C., Discussion - Trans. ASME, J. Appl. Mech., 34, Series E, No. 1, p. 248, (1967).

XII. VITA

Thomas Lanard Paxson, son of Mr. and Mrs. Harry C. Paxson, was born on 22 January 1946, in Coatesville, Pennsylvania. He attended Octorara Area High School, graduating in June of 1963.

The following autumn he began studies at the University of Delaware, Newark, Delaware, in a program resulting in the degree of Bachelor of Mechanical and Aerospace Engineering in June 1967. At that time Mr. Paxson was also commissioned a Second Lieutenant in the United States Army.

In September 1967, Mr. Paxson entered a graduate program at Lehigh University under an NDEA fellowship. He completed his program for a Master of Science Degree in Mechanical Engineering in April of 1969, and left the University to fulfill his military obligation with the United States Army Corps of Engineers.